Biomedicine & Pharmacotherapy 193 (2025) 118791

Contents lists available at ScienceDirect

Biomedicine & Pharmacotherapy

journal homepage: www.elsevier.com/locate/biopha

Cannabidiol modulates brain molecular alterations, gut microbiota dysbiosis and alcohol self-administration in a mouse model of fetal alcohol spectrum disorder

F. Navarrete [a,b,c], R. Cabrera-Rubio [d], A. Gasparyan [a,b,c], R. Aarnio [e,f], F. López-Picón [e,f], S. Helin [g], J. Rajander [g,h], M.C. Collado [d], J. Manzanares [a,b,c,*]

[a] Instituto de Neurociencias, Universidad Miguel Hernández-CSIC, San Juan de Alicante, Alicante, Spain
[b] Instituto de Investigación Sanitaria y Biomédica de Alicante (ISABIAL), Alicante, Spain
[c] Red de Investigación en Atención Primaria de Adicciones (RIAPAd), Instituto de Salud Carlos III, MICINN and FEDER, Madrid, Spain
[d] Institute of Agrochemistry and Food Technology-National Research Council (IATA-CSIC), Valencia, Spain
[e] Preclinical Imaging Laboratory, Turku PET Centre, University of Turku, Turku, Finland
[f] MediCity Research Laboratories, University of Turku, Turku, Finland
[g] Turku PET Centre, University of Turku, Turku, Finland
[h] Åbo Akademi University, Turku, Finland

ARTICLE INFO

Keywords:
Fetal alcohol spectrum disorder (FASD)
Cannabidiol (CBD)
Emotional behavior
Brain biomarkers
Gut microbiota
Alcohol addiction

ABSTRACT

Fetal Alcohol Spectrum Disorder (FASD) is a range of neurodevelopmental abnormalities caused by Perinatal Alcohol Exposure (PAE), leading to profound behavioral and molecular disturbances in the offspring. Unraveling the central and peripheral mechanisms involved, including the microbiota-gut-brain axis, is crucial to improving our understanding of the disease and developing new treatment strategies from a sex perspective. In this study, we investigated the impact of PAE on emotional behavior, brain biomarkers, and gut microbiota composition and diversity in a preclinical C57BL/6 J mouse model, as well as the extent of their vulnerability to alcohol consumption. Furthermore, we have also explored the potential modulatory effects of cannabidiol (CBD) administered chronically (30 mg/kg/day, i.p.) from weaning on PAE-induced sex-dependent emotional and brain molecular impairments, gut microbiota dysbiosis, and increased alcohol reinforcing and motivational actions. FASD model mice showed increased anxiety- and depressive-like behavior accompanied by sex-dependent changes in synaptic density, dopamine D2/D3 receptors availability, cannabinoid receptors 1 and 2 (*Cnr1/Cnr2*), tyrosine hydroxylase (*Th*), and serotonin transporter (*Slc6a4)* gene expression, and gut microbiota dysbiosis. Interestingly, CBD sex-dependently improved and/or normalized PAE-induced behavioral and molecular disturbances. In addition, females but not males exposed to the animal model of FASD showed a higher motivation to drink alcohol, which CBD abolished. Our findings provide new insights into the brain and gut microbiota sex-dependent mechanisms involved in FASD pathophysiology and further highlight the therapeutic potential of CBD to improve the management of FASD-induced emotional disturbances and alcohol addiction from a sex-oriented approach.

1. Introduction

Fetal Alcohol Spectrum Disorder (FASD) is a range of neurodevelopmental abnormalities caused by Perinatal Alcohol Exposure (PAE). Symptoms include deficits in cognitive state, social behavior and emotional regulation, among others [1,2]. Recent reports have shown that PAE is significantly linked to an increased vulnerability to developing a substance use disorder. This may be due to impaired dopaminergic mesolimbic system function [3,4], emphasizing the increased motivation towards alcohol consumption [5,6].

The pathophysiology of FASD is complex and multifactorial. It involves direct neurotoxic effects of ethanol on the developing brain, as well as systemic consequences such as oxidative stress, immune activation and altered neuroendocrine signalling [7,8]. Despite the

* Correspondence to: Instituto de Neurociencias, Universidad Miguel Hernández-CSIC, Avda. Ramón y Cajal s/n, San Juan de Alicante, Alicante 03550, Spain.
E-mail address: jmanzanares@umh.es (J. Manzanares).

https://doi.org/10.1016/j.biopha.2025.118791
Received 7 September 2025; Received in revised form 5 November 2025; Accepted 18 November 2025
Available online 21 November 2025

significant impact of FASD, there are no approved pharmacological treatments capable of reversing FASD-related neurodevelopmental deficits. Current therapeutic strategies primarily focus on symptom management rather than on addressing the underlying neuropathophysiology [9]. In this context, the endocannabinoid system (ECS) has emerged as a promising target for mitigating PAE-induced brain damage. Previous evidence suggests that PAE alters key components of the ECS, including cannabinoid receptors, endocannabinoid ligands, and enzymes that regulate them, leading to neurobehavioral abnormalities [10,11].

Cannabidiol (CBD), a non-addictive constituent of the *Cannabis sativa* plant [12], has demonstrated therapeutic potential due to its multifaceted interactions with various receptors, including CB1 and CB2 cannabinoid receptors, serotonergic receptors (5-HT1A), vanilloid receptors (TRPV1), or peroxisome proliferator-activated receptors (PPARs) [13,14]. Preclinical research suggests that CBD exhibits anxiolytic [15,16], antidepressant [17,18], neuroprotective [19,20], and antiaddictive properties [21,22], showing a significant reduction of the rewarding effects of ethanol [23–26], making it a compelling candidate for FASD treatment. Indeed, a previous study from our laboratory demonstrated that CBD significantly repairs FASD-induced behavioral and molecular alterations in the brains of male and female mice [27]. CBD also attenuated cognitive deficits and neuroinflammation in a rodent model of early alcohol exposure [28]. However, the precise biological mechanisms underlying the modulation of FASD-related emotional and neurobiological dysfunctions by CBD remain largely unclear. Thus, further research is required to investigate the therapeutic potential of CBD and the targets underlying its beneficial effects in FASD.

In recent years, increasing attention has been given to the role of the gut microbiota in brain development and function via the microbiota-gut-brain axis. This is a bidirectional communication system relating intestinal microbes with neural, endocrine, and immune pathways [29,30]. Dysbiosis, or the disruption of the gut microbial ecosystem, has been detected in various neuropsychiatric and neurodevelopmental disorders [31,32]. Notably, chronic alcohol exposure induces gut microbial dysbiosis, reducing the populations of beneficial bacteria, such as *Bifidobacterium*, and increasing intestinal permeability. This fact leads to systemic inflammation and behavioral abnormalities [33,34], effects that can be improved by interventions targeting the microbiota [35,36]. Despite these promising findings, the effects of PAE on gut microbiota composition remain poorly explored [37,38], particularly in the context of long-term developmental outcomes in the offspring [39]. Importantly, sex-specific differences in gut microbiota have been reported [40,41]; however, these factors are often overlooked in microbiome research.

In this study, we investigated the impact of PAE on emotional behavior, brain synaptic density, central biomarkers, and gut microbiota composition and diversity in male and female adolescent offspring, and their vulnerability to alcohol consumption and motivation. Furthermore, we have also explored the potential modulatory effects of CBD administered from weaning (postnatal day 21, PND21) on PAE-induced behavioral and brain molecular impairments. To our knowledge, this is the first study evaluating whether long-term CBD administration can reverse or mitigate gut microbiota alterations induced by PAE. We assessed taxonomic shifts, diversity metrics, and functional correlations across control, FASD, and FASD-CBD groups using 16S rRNA sequencing and explored sex-dependent differences in the microbial community. Our results provide novel insights into the interplay between ethanol exposure, gut microbiota, and CBD intervention, and highlight potential microbial biomarkers and therapeutic targets for FASD.

2. Materials and methods

2.1. Animals

We used C57BL/6 J male and female mice in all experiments. Fifty female and 20 male 5-week-old mice were purchased from Charles River Laboratories (Lille, France). After their arrival, the mice were individually housed and left undisturbed for one week to acclimate to the animal housing room. Subsequently, females were exposed to a voluntary ethanol consumption paradigm before breeding initiation. A total of 168 offspring (84 males and 84 females) were obtained from the cross-breeding. The mice were group-housed in cages divided by sex (males (M) and females (F)) and experimental condition according to perinatal exposure to water (H_2O) or ethanol (EtOH), as well as the pharmacological treatment initiated on postnatal day 21 (PND21) with CBD or its corresponding vehicle (VEH). Thus, the experimental groups were as follows, per sex: H_2O-VEH, EtOH-VEH, and EtOH-CBD. All animals were maintained in the Animal Facilities Service of the Universidad Miguel Hernández (SEA-UMH) under controlled environmental conditions of temperature (23 ± 2 °C), humidity (60 ± 10 %), and a 12-h light-dark cycle (lights on from 08:00–20:00 h). All experimental procedures complied with the Spanish Royal Decree 53/2013, the Spanish Law 32/2007, and the European Union Directive of 22 September 2010 (2010/63/UE) regulating the care of experimental animals and were approved by the Ethics Committee of Miguel Hernández University. Animal studies are reported in compliance with the ARRIVE guidelines [42].

2.2. Perinatal Alcohol Exposure (PAE)

As previously described, female C57BL/6 J mice were exposed to voluntary ethanol consumption in a two-bottle choice paradigm from PND 42 [27]. After an acclimation period, animals were divided into two groups, one exposed to two bottles containing tap water (n = 15), and another exposed to one bottle containing tap water and the other containing increasing ethanol concentrations (2.5, 5, 7.5, and 10 % of ethanol, 3 days each concentration until stabilization at 10 %) (n = 35). The volumes of ethanol and water consumed were carefully measured and filled daily to calculate the ethanol consumption (g/kg/day) and the ratio of ethanol preference [ethanol preference: ethanol intake / (ethanol intake + water intake)]. Once the 10 % ethanol consumption and preference were stabilized for 15 days (or the equivalent period of water access in control animals), vaginal smears were collected in the afternoon for cytological evaluation, selecting only females with high ethanol consumption and preference (for more details see Gasparyan et al. [27]). At this point, 30 females from the initial 35 were selected and were crossed with singly housed males when they were at the pro-estrus or estrus stages. From GD7 until PND21, mothers previously exposed to voluntary ethanol consumption were administered 3 g/kg of ethanol (p.o., twice a day). In contrast, those not exposed to ethanol received tap water (p.o., twice a day) (Fig. 1). In the group of ethanol-exposed females, only 18 finished gestation and lactation periods appropriately, whereas in the control group, 10 of the initial 15 females did so.

2.3. Cannabidiol (CBD) treatment of offspring exposed perinatally to alcohol

CBD was acquired from THC Pharm (Frankfurt, Germany) and dissolved in a solution of ethanol, cremophor and saline (1:1:18) to achieve the selected dose of 30 mg/kg. This dose was chosen in conjunction with the beginning of CBD administration at PND21, in line with our previous findings using the same animal model of FASD [27]. In this study, CBD at a dose of 30 mg/kg, administered from PND21 onwards, was found to significantly improve behavioral, molecular, and cellular parameters affected by PAE. The drug was prepared daily immediately before its administration (between 17:00 and 19:00 h) at a volume of 10 mL/kg.

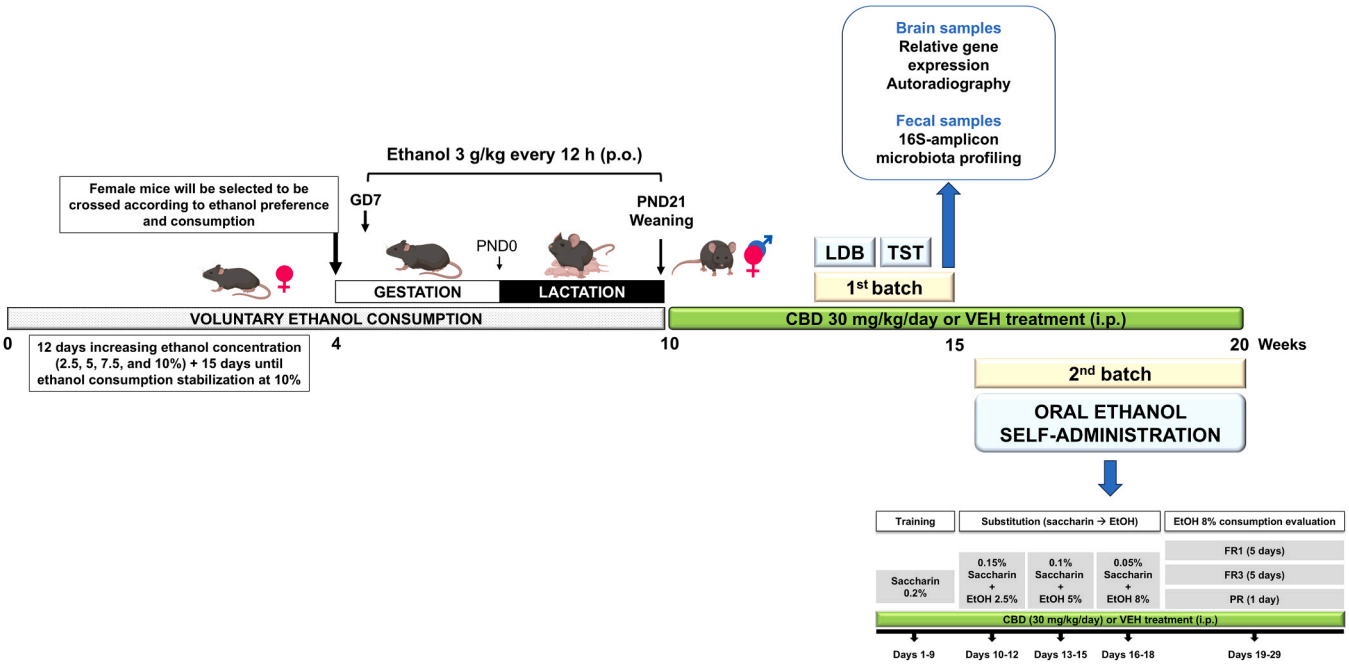

Fig. 1. Schematic diagram showing the design of the experimental procedures. Female mice were exposed to a voluntary ethanol consumption paradigm, achieving stable ethanol consumption and preference at 10 % before crossing. After gestation confirmation, at GD7, ethanol gavage was started at a dose of 3 g/kg/12 h (p.o.) until the pup's weaning at PND21. Pups were treated with CBD (30 mg/kg/24 h, i.p.) or VEH from the day of weaning for 5 (1st batch) or 10 (2nd batch) weeks. In the 1st batch, after the 4th week of treatment, behavioral evaluations were performed in male and female animals to determine the effects of CBD on anxiety and depressive symptoms using the light-dark box (LDB) and tail suspension test (TST), respectively. At the end of these behavioral studies, mice were killed by cervical dislocation, obtaining brain and fecal samples that were frozen for their use in the study of the gene, autoradiography, and microbiota profiling analyses. In the 2nd batch, after the 6th week of treatment, oral ethanol self-administration was performed in male and female animals to evaluate the effects of CBD on ethanol's reinforcing and motivational actions. CBD: cannabidiol, FR1: fixed ratio 1 schedule, FR3: fixed ratio 3 schedule, GD: gestational day, i.p.: intraperitoneal administration, LDB: light-dark box, PND: postnatal day, p.o.: oral administration, PR: progressive ratio, TST: tail suspension test, VEH: vehicle.

The daily treatment with CBD at 30 mg/kg or vehicle (VEH) (i.p.), the latter also composed of a mixture of ethanol, cremophor and saline in a ratio of 1:1:18, was initiated on the same day as weaning, when the offspring from the crossbreeding were separated by sex and housed in groups of 4–6 mice per cage. The emotional behavioral evaluation started after 4 weeks from the beginning of treatment with CBD, which continued approximately up to 10 weeks, until the end of the oral ethanol self-administration (OEA). First, CBD effects on anxiety and depressive-like behaviors were analyzed by the light-dark box (LDB) and tail suspension test (TST), respectively, which were performed during week 14, as well as the effect of CBD on brain relative gene expression, dopamine D2/D3 receptors and synaptic density analyzed from brain slice autoradiography, and fecal 16S-amplicon microbiota profiling (week 15). Second, ethanol consumption and motivation were evaluated by the OEA paradigm from weeks 16–20 (Fig. 1).

2.4. Emotional behavior evaluation

2.4.1. Light-dark box (LDB)

Anxiety-like behaviour was evaluated by the widely accepted LDB paradigm. LDB was carried out in an apparatus with two methacrylate compartments (20 ×20 x 15 cm), one transparent and the other black and opaque, separated by an opaque tunnel (4 cm). The light compartment is illuminated with a lamp (60 W) that is placed 25 cm above it. At the beginning of the 5-minute session, mice were placed in the light box facing the tunnel. The total time spent in the light box and the number of transitions between boxes were recorded. A mouse whose four paws were inside the new box was considered to have changed boxes.

2.4.2. Tail suspension test (TST)

TST is a widely accepted test to assess rodent depressive-like behaviors. Mice were individually suspended by the tail at the edge of a lever suspended above the tabletop (35 cm), with adhesive tape placed approximately 1–2 cm from the tail tip. The immobility time was measured for 6 min.

2.5. Mice samples for molecular studies

At the end of the emotional behavior evaluation (week 15, PND56), and 14–16 h after the last drug administration (CBD or VEH), a batch of mice was sacrificed by cervical dislocation to obtain: 1) frozen brain samples for relative gene expression (n = 7–9 animals/group) and *in vitro* radiotracer autoradiography (n = 6–8 animals/group) analyses; and 2) frozen fecal samples for microbiota profiling by 16S rRNA amplicon sequencing (n = 12–14 animals/group) (Fig. 1).

2.6. Autoradiography studies

For the *in vitro* autoradiography studies, 20 μm slices were prepared from all the brains using a cryostat (Leica CM3050S, Germany). Two different radiotracers – [^{11}C]UCB-J and [^{11}C]raclopride – were synthesized at the Radiopharmaceutical Chemistry Laboratory of Turku PET Centre and used for in vitro autoradiography studies, with optimized protocols for each.

The changes in synaptic density were studied using the synaptic vesicle glycoprotein 2 A (SV2A) targeting radiotracer [^{11}C]UCB-J [43]. The *in vitro* binding protocol was adapted with some changes from a previous study by Värnas et al. [44]. In short, the brain slices were first pre-incubated in a buffer solution containing 50 mM Tris and 2 mM $MgCl_2$ at 4°C for 5 min and then incubated for 20 min in the same Tris-$MgCl_2$ buffer at room temperature (RT) with 6.1 ± 1.2 nM (0.15 ± 0.01 MBq/mL) of [^{11}C]UCB-J. Following incubation with [11 C] UCB-J, the slices were rinsed twice for 5 min in the same Tris-MgCl2 buffer at 4°C, then quickly rinsed in reverse osmosis-purified water

(RO H_2O) at 4 °C.

To detect changes in dopamine D2/D3 receptors, we used the radioligand [^{11}C]raclopride [45]. The brain slices were first pre-incubated in a buffer solution containing 50 mM Tris and 120 mM NaCl (pH 7.4) at RT for 30 min. Afterwards, the slices were incubated for 20 min in the same Tris-NaCl buffer at RT with 1.6 ± 0.4 nM (0.11 ± 0.03 MBq/mL) of [^{11}C]raclopride. Following the incubation with [^{11}C]raclopride, the slices were rinsed 3 × 5 min in the same buffer at 4°C, and then quickly rinsed in RO H_2O at 4°C.

After the *in vitro* binding protocol for [^{11}C]UCB-J and [^{11}C]raclopride, the slices were air-dried and exposed to a phosphor imaging plate (Fuji BAS Imaging Plate TR2025, Fuji Photo Film Co., Ltd., Tokyo, Japan) for about two half-lives (approximately 40 min). After exposure, the imaging plates were scanned with a BAS-5000 phosphorimager (Fuji, Japan) at 25 μm resolution and analyzed with AIDA Image Analyzer 4.5 (Raytest, Isotopenmessgeräte, Straubenhardt, Germany).

2.7. Relative gene expression analyses by quantitative real-time PCR

Relative gene expression of cannabinoid receptors 1 (*Cnr1*) and 2 (*Cnr2*) in the nucleus accumbens (NAcc), tyrosine hydroxylase (*Th*) in the ventral tegmental area (VTA), and serotonin transporter (*Slc6a4*) in the dorsal raphe (DR) was analyzed by real-time polymerase chain reaction (RT-PCR). For that purpose, brains were removed from the skull and frozen at −80ºC. These samples were cut in a cryostat (-10ºC), obtaining coronal sections of 500 μm following the atlas of Paxinos and Fraklin [46]. They were microdissected following the procedure described by Palkovits and previously performed by our group [47]. Total ribonucleic acid (RNA) was extracted with TRI Reagent extraction, and reverse transcription was carried out (Applied Biosystems, Madrid, Spain). Quantitative analyses of the relative gene expression of *Cnr1* (Mm00432621_s1), *Cnr2* (Mm00438286_m1), *Th* (Mm00447546_m1), and *Slc6a4* (Mm0043939_m1) genes were performed on the StepOne Sequence Detector System (Applied Biosystems, Madrid, Spain). Data for each target gene were normalized to the endogenous reference gene 18S (Mm03928990_g1), and the fold change in target gene expression was determined using the 2-ΔΔCt method [48].

2.8. Microbiota profiling by 16S rRNA amplicon sequencing

The total DNA was isolated from the fecal samples using the MasterPure DNA Extraction Kit (Epicentre, Madison, WI, USA) according to the manufacturer's instructions, with some modifications, including physical and enzymatic treatments. The V3–V4 variable region of the 16S rRNA gene was sequenced using Illumina protocols to determine fecal microbiota composition and diversity. A Nextera XT Index Kit (Illumina, CA, USA) was used for multiplexing, and a Bioanalyzer DNA 1000 chip (Agilent Technologies, CA, USA) was used to assess the quality of the polymerase chain reaction (PCR) product. Libraries were sequenced using a 2 × 300 bp paired-end run (MiSeq Reagent Kit v3) on a MiSeq-Illumina platform (FISABIO Sequencing Service, Valencia, Spain), according to the manufacturer's instructions (Illumina).

Bioinformatic analysis of bacterial diversity was performed following stringent procedures. Raw reads were quality and length checked (removal of low-quality nucleotides at the 3' end in windows of 20 nt with a low average quality and removal of sequences with less than 200nt) with the Fastp program [49]. In addition, fastp was used for adapter removal and deduplication, as well as for eliminating sequences shorter than 200 nucleotides. The paired-end reads with a minimum overlap of 30 bp were joined using Fastq-join [50]. Sequences were trimmed of primers and distal bases, and singletons were removed with USEARCH v11 [51]. zOTUs (zero-radius operational taxon units) mapping to the human genome (GRCh38) using the Burrow–Wheeler Aligner in Deconseq v0.4.3 were filtered out [52]. The resulting reads were denoised, and chimeras were filtered with UNOISE3 [53]. The samples were filtered, resulting in fewer than 30,000 reads for the final data analysis. Taxonomic assignment of zOTUs was performed in QIIME 2 v2018.2 [54] using the QIIME 2 feature classifier plugin [55] and the Ribosomal Database Project (RDP) [56]. For nomenclature consistency, genus-level taxa are reported verbatim as returned by the RDP Naïve Bayesian Classifier (trainset v2.14)—including labels such as Clostridium XIVa, Clostridium XIVb, Clostridium XVIII, and Clostridium sensu stricto—and no post hoc remapping or synonym consolidation was performed. Reads classified as mitochondria and chloroplasts were removed before statistical analysis. The zOTUs were aligned using MAFFT [57] to create a phylogenetic tree with FASTTREE [58], which was midpoint rooted. To reduce compositional biases, downstream analyses combined relative-abundance summaries with compositional data methods (centered log-ratio and genus balances). Taxa retained for inference met prevalence (≥25 % of samples) and abundance (≥0.01 %) thresholds to limit spurious low-count effects.

2.9. Oral ethanol self-administration (OEA)

OEA was performed following a previously published protocol by our group [59] to evaluate the effects of CBD in a second batch of male and female offspring on ethanol reinforcement and motivation. The OEA was conducted in 18 modular operant chambers (Panlab) located within 18 noise-isolation boxes, each equipped with a chamber light, two levers, a receptacle for dropping liquid solutions, a syringe pump, a stimulus light, and a buzzer. Packwin software (Panlab) controlled stimulus and fluid delivery and recorded operant responses.

Pressing on one of the levers did not have any consequence (inactive lever), whereas pressing the other lever (active lever) delivered 36 μl fluid combined with a 0.5 s bright stimulus and a 0.5 s, 2850 Hz, 85 dB buzzer beep, followed by a time-out period of 6 s, in which no fluid was delivered. After the 6-second time-out, an intertrial interval (ITI) started, the duration of which depended on each subject's spontaneous waiting before an active lever press. The experiment was divided into three phases: training, saccharin substitution and ethanol 8 % (*v/v*) consumption (see Fig. 1).

Training phase (9 days): Two days before the experiment, standard chow was restricted to 1 h of access per day. Before the first training session, water access was restricted for 24 h to increase the motivation for lever pressing according to protocols previously described [23, 59–63]. During this deprivation period, no behavioural or physical decline was observed. The body weight fluctuation was never higher than 10 %. A food allotment was provided 1 h before the 60-minute session, also to increase motivation for lever pressing. During the subsequent four days, water was provided *ad libitum*, except during a 1-hour period immediately before the start of each session, when the water bottle was removed from the cages (postprandially). For the next five days and throughout the remainder of the experiment, food access was restricted only during the dark cycle (from 8:00 p.m.–8:00 a.m.), and water was available ad libitum to prevent ethanol consumption due to thirst (preprandial). Male and female offspring perinatally exposed to ethanol were trained to press the active lever to receive 36 μL of 0.2 % (*w/v*) saccharin as reinforcement.

Saccharin substitution (9 days): The saccharin concentration was gradually decreased as the ethanol concentration was gradually increased [64]. Each solution combination was assigned to three consecutive sessions (0.15 % Sac–2.5 % EtOH, 0.10 % Sac–5 % EtOH, 0.05 % Sac–8 % EtOH).

8 % (v/v) ethanol consumption (11 days): the number of responses on the active lever, the 8 % ethanol (*v/v*) consumption and the motivation to drink in male and female offspring daily treated with CBD (30 mg/kg/day; i.p.) or VEH (i.p.) were measured. There were three phases: 1) Fixed Ratio 1 (FR1), mice responding on the active lever to obtain 8 % ethanol and no saccharin were evaluated using an FR1 reinforcement schedule during 5 daily consecutive 1 h sessions; 2) Fixed Ratio 3 (FR3), after FR1 mice underwent 5 daily 1 h sessions using an FR3 reinforcement schedule (mice have to respond three times on the active lever to achieve

one reinforcement); and 3) Progressive Ratio (PR), on the day after FR3, a PR session was carried out. In this session, the response requirement to earn reinforcements escalated according to the following series: 1, 2, 3, 5, 12, 18, 27, 40, 60, 90, 135, 200, 300, 450, 675, 1000. The PR session lasted for 2 h, and the 'breaking point' (the maximum number of lever presses each animal can perform to achieve one reinforcement) was determined in each animal.

2.10. Statistical analysis and prediction models

2.10.1. Behavioral and brain molecular results

Statistical analyses were performed using SigmaPlot 11.0 for all data, except for microbiota profiling (see the corresponding section below). The Student's *t*-test was used to compare two groups, and one-way analysis of variance (ANOVA) was used to compare three groups, followed by the Student-Newman-Keuls' test for post hoc analyses. Differences were considered significant if the type 1 error (alpha) probability was less than 5 %. For transparency and robustness, all main ANOVA findings were additionally verified using Tukey's HSD, and families of planned contrasts/correlations were controlled by FDR (Benjamini–Hochberg), yielding the same inferential conclusions. Associations between microbiota and neurobehavioral variables were treated as exploratory and correlational; no causal inferences were drawn from these analyses.

2.10.2. Microbiota profiling results

The alpha-diversity indices (Chao1, Simpson, and Shannon) were calculated for each sample using the phyloseq R package [65], and differences between groups were assessed using ANOVA. PERMANOVA test from vegan R package [66] evaluated overall differences in microbiota structure using a Bray-Curtis and unweighted Unfrac distance matrix zOTUs analysis and beta-diversity plots. Rarefied was not performed; however, a filter of 0.01 % relative abundance in at least 25 % of the samples was established to conduct the following analyses. A balanced selection has been performed on microbiota composition data. In addition, a linear discriminant analysis effect size (LefSe) was performed to identify specific bacterial biomarkers associated with the studied groups. Shapiro-Wilk for normality, guided test selection; when violated, we applied data transformations or non-parametric alternatives. We also implemented two additional compositional data analysis algorithms to define which features were significantly unbalanced among groups (EtOH-VEH vs H_2O-VEH, EtOH-VEH vs EtOH-CBD, and EtOH-CBD_M vs EtOH-CBD_F). We implemented the CLR-lasso [67] methods as described in https://malucalle.github.io/Microbiome-Variable-Selection/ to detect a type of microbial signature between groups, potentially. Using the same R package, we created a Selbal-like plot. The top panel lists the selected genus with either negative (B) or positive (A) coefficients. The names are ordered according to their importance (absolute coefficient values). The middle boxplots are based on the log mean difference between the negative and positive variables: $1p+ \Sigma p + i = 1 \log (Xi)$ - $1p\text{-}\Sigma p\text{-}j = 1 \log (Xj)$. This log mean difference is calculated for each sample as a balance score, which is proportional to the balance reported in Rivera-Pinto et al., 2018 [68].

All assumption checks and model selection steps were conducted a priori during data analysis and are made explicit here for transparency: normality was assessed with Shapiro-Wilk and variance homogeneity with Levene (or Brown-Forsythe when appropriate); when assumptions were violated, we applied log/Box–Cox transformations or used non-parametric tests (Mann–Whitney or Kruskal-Wallis with FDR-controlled pairwise comparisons). Where design and group sizes allowed, we additionally fit two-way ANOVAs (Sex × Group/Treatment). In addition, to relate behavioral outcomes with brain markers, we computed sex-stratified Pearson/Spearman correlations and hierarchical linear models in which emotional (LDB, TST) and OEA (FR1, FR3, PR) measures were predicted by autoradiography ratios ([^{11}C]UCB-J, [^{11}C]raclopride) and gene expression (Cnr1, Cnr2, Th, Slc6a4), including treatment (VEH vs CBD) and PAE status as fixed factors and their interactions. Unless otherwise specified, families of related p-values were adjusted by FDR.

To integrate microbiota with brain and behavior, we performed constrained ordination (RDA with Bray–Curtis) including neurobehavioral variables (LDB, TST, FR1/FR3/PR; [^{11}C]UCB-J; [^{11}C] raclopride ratios; Cnr1/Cnr2/Th/Slc6a4) as environmental drivers (envfit) [80]. We additionally computed genus-level Spearman correlations with neurobehavioral variables, controlling for multiple testing (Benjamini–Hochberg) and, where helpful, summarized group differences using log-ratio "balances" (Selbal-like) to obtain interpretable composite biomarkers. Analyses were performed within a compositional framework when appropriate (e.g., the CLR transformation for correlation/ordination sensitivity checks). To avoid overstating mechanistic links, ordination biplots and correlation heatmaps were interpreted as associations without directionality."

3. Results

3.1. Emotional behavior alterations induced by PAE and improvement induced by CBD administration

The LDB test revealed a significant reduction in time spent in the lighted box in males and females exposed to ethanol during the perinatal period compared with water-exposed animals. In both sexes, CBD administration completely normalized these decreases (Fig. 2**A**; Males, One-way ANOVA, $F_{[2,29]} = 3.842$, $P = 0.034$; Fig. 2**B**; Females, One-way ANOVA, $F_{[2,29]} = 4.843$, $P = 0.017$). No changes were found in the number of transitions in either males (Fig. 2**C**; One-way ANOVA, $F_{[2,29]} = 0.424$, $P = 0.659$) or females (Fig. 2**D**; One-way ANOVA, $F_{[2,29]} = 0.319$, $P = 0.730$).

In the TST, animals that experienced PAE showed increased immobility time compared with controls, with a greater effect in females. Interestingly, CBD treatment significantly reduced immobility time, achieving values similar to those of the control group in both sexes (Fig. 2**E**; Males, One-way ANOVA, $F_{[2,29]} = 4.492$, $P = 0.022$; Fig. 2**F**; Females, One-way ANOVA, $F_{[2,29]} = 14.352$, $P < 0.001$).

3.2. PAE-induced changes in [11C]UCB-J and [11C]Raclopride binding assessed by autoradiography and effects observed with CBD treatment

Autoradiography studies for the [^{11}C]UCB-J in the cortex and HIPP revealed reduced uptake in both brain regions in males exposed to the FASD model and treated with vehicle or CBD (Males; Fig. 3**C**, One-way ANOVA, $F_{[2,20]} = 9.762$, $P = 0.001$; Fig. 3**E**, One-way ANOVA, $F_{[2,20]} = 9.285$, $P = 0.002$). However, no differences were observed in females in the cortex (Fig. 3**D**, One-way ANOVA, $F_{[2,22]} = 1.258$, $P = 0.306$) nor in the HIPP (Fig. 3**F**, One-way ANOVA, $F_{[2,22]} = 3.135$, $P = 0.065$). On the other hand, in the [^{11}C]raclopride autoradiography studies, FASD model-exposed males (but not females) showed a reduced binding ratio of striatum to cortex which was modulated after the early and chronic CBD administration (Fig. 3**G**; Males, One-way ANOVA, $F_{[2,22]} = 11.195$, $P < 0.001$; Fig. 3**H**; Females, One-way ANOVA, $F_{[2,23]} = 2.994$, $P = 0.072$). Interestingly, the ratio of accumbens to cortex of the uptake of [^{11}C] raclopride was increased in female mice exposed to the FASD model and normalized with CBD administration. However, no changes were found in the same brain region of male mice (Fig. 3**I**; Males, One-way ANOVA, $F_{[2,22]} = 0.809$, $P = 0.459$; Fig. 3**J**; Females, One-way ANOVA, $F_{[2,23]} = 6.995$, $P = 0.005$).

3.3. PAE-induced changes in the relative gene expression of Cnr1, Cnr2, Th, and Slc6a4 and modulatory effects of CBD administration

Gene expression studies in the Nacc revealed a statistically reduced basal gene expression of *Cnr1* in females compared with males (Fig. 4**A**; Student's *t*-test, $t = 3.057$, $P = 0.009$, 14 d.f.). In males, exposure to the

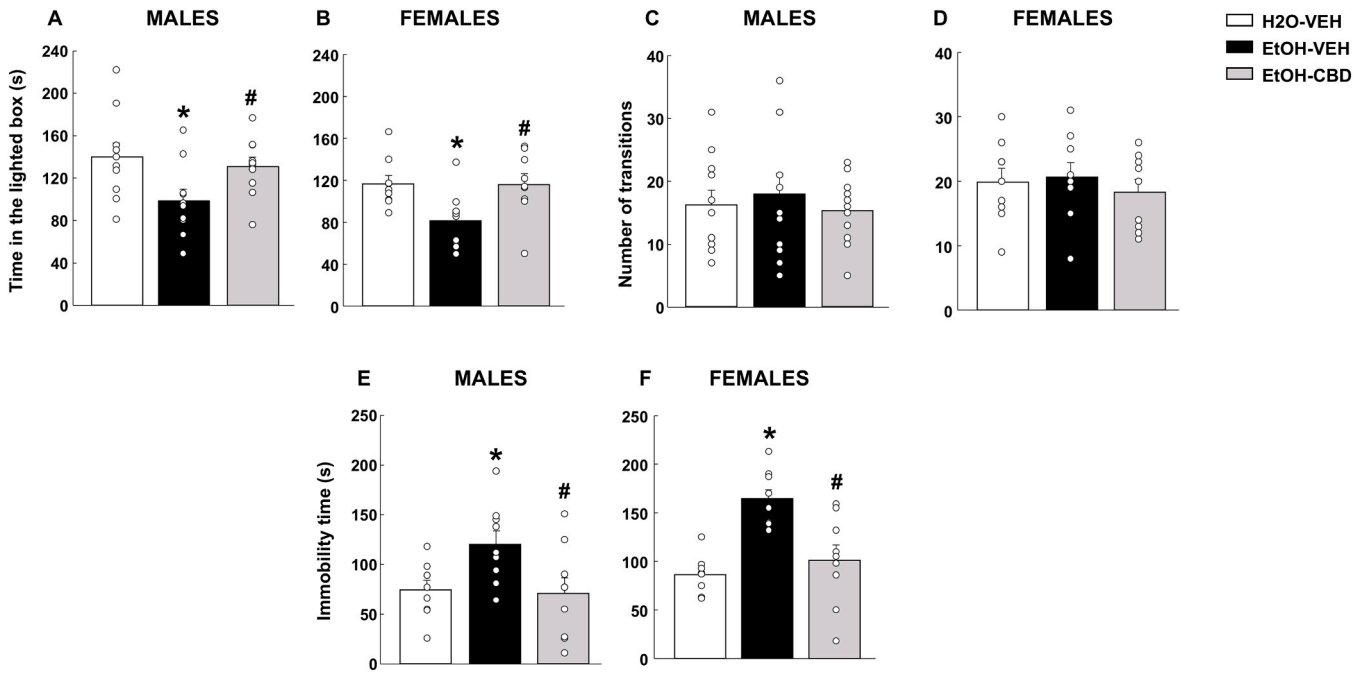

Fig. 2. Evaluation of the emotional alterations in male and female mice perinatally exposed to ethanol and chronically treated with CBD (30 mg/kg/24 h, i.p.). Immediately after weaning and for the next 4 weeks, mice were treated with CBD or VEH. During week 5, the emotional state and the effects of CBD were evaluated. Anxiety- and depressive-like behaviors were analyzed by the light-dark box (time in the lighted box: A and B, number of transitions: C and D; n = 10/group) and the tail suspension test (E and F; n = 10/group), respectively. * $P < 0.05$ vs H_2O-VEH group; # $P < 0.05$ vs EtOH-VEH group.

FASD model increased the gene expression of this target, which was normalized in the CBD-treated group (Fig. 4**B**; One-way ANOVA, F [2, 23] = 8.785, P = 0.002). In females, a slight increase in *Cnr1* gene expression was also detected, although it was not modulated with CBD administration (Fig. 4**C**; One-way ANOVA, F [2,23] = 6.096, P = 0.008).

Basal *Cnr2* gene expression levels in the NAcc were higher in females than in males (Fig. 4**D**; Student's *t*-test, t = -4.665, P < 0.001, 14 d.f.). Male mice exposed to the FASD model showed a significant increase in Cnr2 gene expression compared to controls, with a greater effect in males than in females. Interestingly, CBD treatment completely normalized this FASD-induced alteration in males but not in females (Fig. 4**E**; Males, One-way ANOVA, F [2,23] = 5.086, P = 0.017; Fig. 4**F**; Females, One-way ANOVA, F [2,23] = 4.519, P = 0.023).

In the VTA, under basal conditions, *Th* gene expression was lower in females than in males (Fig. 4**G**; Student's *t*-test, t = 2.257, P = 0.042, 14 d.f.). In males, PAE reduced the gene expression of this target, which was normalized in mice treated with CBD (Fig. 4**H**; One-way ANOVA, F [2, 23] = 10.293, P < 0.001). In contrast, the exposure to the FASD model in females increased the gene expression of *Th*, which was not modified after CBD administration (Fig. 4**I**; One-way ANOVA, F [2,23] = 5.874, P = 0.010).

Finally, relative gene expression of *Slc6a4* in the DR of VEH-treated animals was upregulated in females compared with males (Fig. 4**J**; Student's *t*-test, t = -3.926, P = 0.002, 14 d.f.). Exposure to ethanol during gestation and lactation significantly increased Slc6a4 gene expression in the DR, with levels approximately twice as high in males as in females. Interestingly, CBD normalized the elevated *Slc6a4* gene expression levels in both sexes (Fig. 4**K**; Males, One-way ANOVA, F [2, 23] = 4.327, P = 0.024; Fig. 4**L**; Females, One-way ANOVA, F [2,23] = 5.901, P = 0.008).

3.4. Gut microbiota profiling

3.4.1. General description of all groups of samples

In all experimental groups, the gut microbiota composition was primarily dominated by zOTUs from the phyla Bacteroidetes (Bacteroidota), Verrucomicrobia, Firmicutes (Bacillota), and Proteobacteria (Pseudomonadota), together accounting for approximately 90 % of the total microbial relative abundance (Fig. 5**A**). At the family level, the most abundant taxa were *Porphyromonadaceae*, *Verrucomicrobiaceae*, *Erysipelotrichaceae*, and *Bacteroidaceae* (Fig. 5**B**). At the genus level, the most prevalent taxa included *Akkermansia*, *Bacteroides*, *Parasutterella*, *Bifidobacterium*, *Alloprevotella*, *Turicibacter*, *Barnesiella*, *Lactobacillus*, *Prevotella*, *Clostridium_XVIII*, *Alistipes*, *Parabacteroides*, *Blautia*, *Helicobacter*, *Olsenella*, and *Escherichia/Shigella* (Fig. 5**C**).

When accounting for sex, bacterial composition remained unchanged at the phylum and family levels. However, at the genus level, notable differences were observed, with the most prevalent genera being *Akkermansia*, *Duncaniella*, *Bacteroides*, *Bifidobacterium*, *Muribaculum*, *Prevotella*, *Dubosiella*, *Ileibacterium*, *Turicibacter*, *Faecalibaculum*, *Paramuribaculum*, *Thomasclavelia*, *Alistipes*, *Turicimonas*, *Lactobacillus*, *Parabacteroides*, *Ligilactobacillus*, *Blautia* and *Helicobacter* (Fig. 5**D**). Together, these patterns establish a stable phylum-level background with room for condition- and sex-specific genus-level remodeling.

These taxonomic patterns were further contextualized by evaluating overall community structure across groups. Principal Coordinates Analysis (PCoA) based on Unifrac unweighted dissimilarity revealed a partial but consistent separation among the experimental groups (Fig. 5**F**). The EtOH-CBD group formed a distinct cluster, clearly separated from both the EtOH-VEH and H2O-VEH groups, explaining 32.5 % of the total variance (PERMANOVA $R^2 = 0.166$, P = 0.027), highlighting that CBD treatment strongly influenced gut microbiota. These results indicate that the overall microbial ecology differs between treatment groups, beyond changes in individual taxa.

3.5. Gut microbiota is influenced by Alcohol and modulated by CBD in a sex-dependent manner, and it is associated with brain-related markers

3.5.1. Gut microbiota between the H_2O-VEH and EtOH-VEH groups are sex-dependent

Alpha diversity analysis (Shannon and Simpson indices) showed no significant differences between groups. However, the diversity in

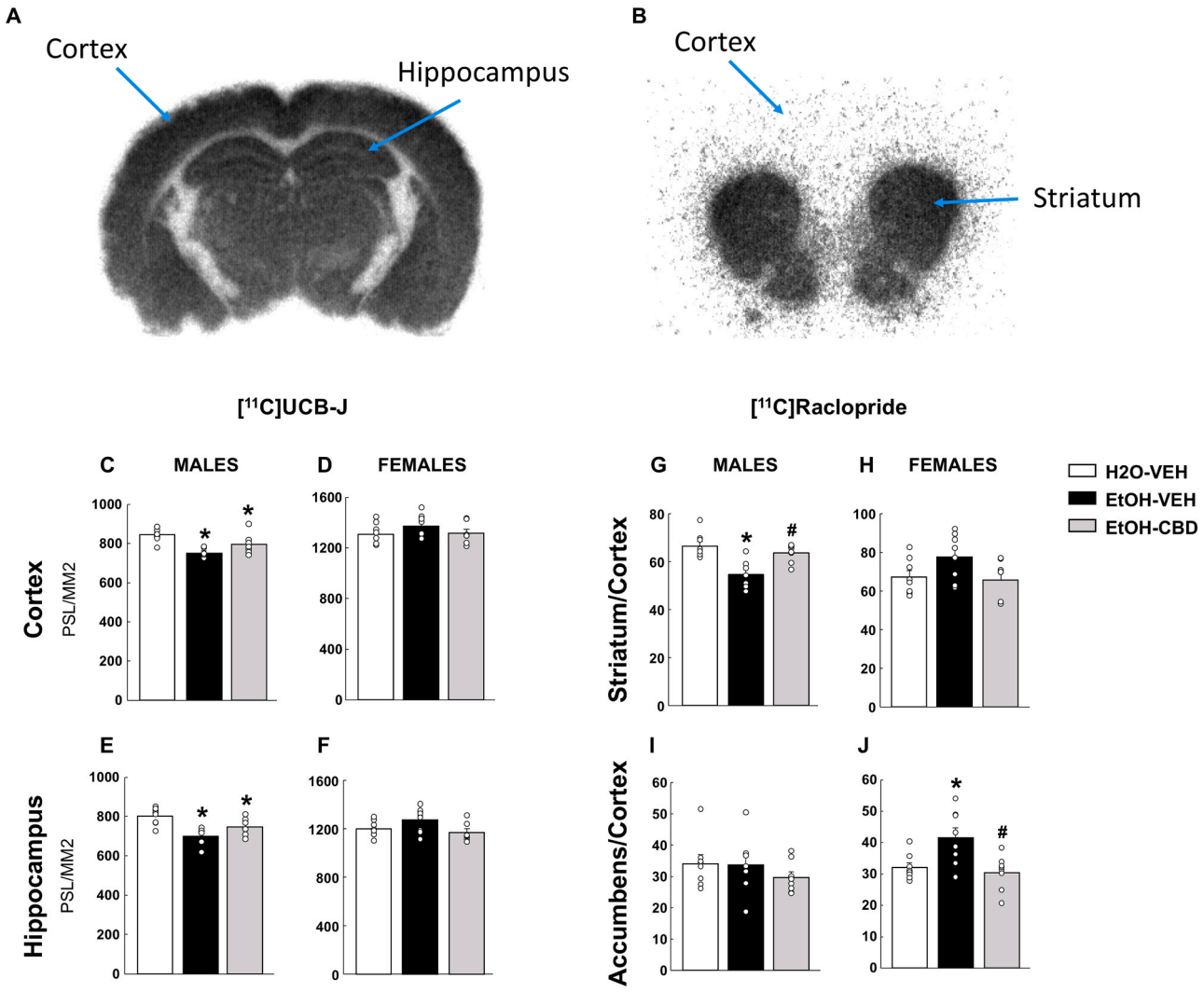

Fig. 3. *In vitro* autoradiographic studies to evaluate synaptic density and D2/D3 receptors availability by measuring [^{11}C]UCB-J and [^{11}C]raclopride binding, respectively, in male and female mice perinatally exposed to ethanol and chronically treated with CBD (30 mg/kg/24 h, i.p.). Representative coronal brain slices, including the regions of interest: cortex and hippocampus for evaluating [^{11}C]UCB-J binding (A); striatum/cortex and accumbens/cortex ratios for detecting [^{11}C] raclopride binding (B). Autoradiography studies for the [^{11}C]UCB-J in the cortex (C and D; n = 6–8/group) and the HIPP (E and F; n = 7–8/group), and for the [^{11}C] raclopride in the striatum/cortex (G and H; n = 7–8/group) and the accumbens/cortex (I and J; n = 7–8/group) ratios. * $P < 0.05$ vs H_2O-VEH group; # $P < 0.05$ vs EtOH-VEH group.

ethanol-exposed samples showed greater variability than in the more stable H_2O_VEH group (Fig. 5**E**). Beta diversity analysis using principal coordinates analysis (PCoA; unweighted) revealed distinct clustering between H_2O and ethanol-exposed groups ($R^2 = 0.18778$, $P = 0.001$) (Fig. 6**A**). Subgroup analysis by sex also indicated significant differences in microbial composition: (A) EtOH-VEH_H vs H_2O-VEH_H ($R^2 = 0.249$, $P = 0.006$), (B) EtOH-VEH_H vs EtOH-VEH_M ($R^2 = 0.159$, $P = 0.021$), and (C) H_2O-VEH_H vs EtOH-VEH_M ($R^2 = 0.121$, $P = 0.030$) (Fig. 6**E**).

Core zOTUS analysis revealed a 31.9 % overlap between the H_2O-VEH and EtOH-VEH groups, with 30.3 % of zOTUs unique to EtOH-VEH and 37.8 % unique to H_2O-VEH (Fig. 7**A**). LEfSe analysis identified differentially abundant taxa, with *Alloprevotella* enriched in H_2O-VEH, and *Bacteroides*, *Clostridium_XVIII*, *Blautia*, *Parabacteroides*, *Rubellimicrobium*, and *Clostridium_XIVa* enriched in EtOH-VEH (Fig. 7**D**). PAE shifted communities toward pro-inflammatory/putative dysbiotic genera, laying the ground for brain–behavior links

To explicitly link community structure with neurobehavioral variation, RDA/envfit identified NA_CB1_Cnr1 ($R^2 = 0.1387$, $P = 0.047$), NA_CB2_Cnr2 ($R^2 = 0.2957$, $P = 0.008$), FR3 ($R^2 = 0.2268$, $P = 0.034$), and VTA_TH ($R^2 = 0.1987$, $P = 0.041$) as significant correlates (Fig. 8D). Along RDA1 (10.7 %), H2O-VEH samples aligned with LDB Time and cortical [^{1} ^{1}C]UCB-J, associated with Turicibacter, Alloprevotella, and Bifidobacterium, whereas EtOH-VEH aligned with DR_5HTT, NA_CB1_Cnr1, PR, NA_CB2_Cnr2, and FR3 and was enriched in Blautia, Parabacteroides, Parasutterella, Bacteroides, Clostridium_XVIII, and Rubellimicrobium (Fig. 8A)

Spearman correlation analysis showed significant associations: *Alistipes* correlated positively with the TST; *Clostridium_XIVa*, *Blautia*, *Parasutterella*, and *Clostridium_XVIII* with PR; *Clostridium_XIVa* with FR3; *Rubellimicrobium* with VTA_TH (negative) and NA_CB2_Cnr2 (positive), along with *Parabacteroides* and *Blautia* (Fig. 8**C**). These results indicate that PAE-linked dysbiosis is not merely compositional but maps onto ECS and monoaminergic markers and motivational readouts, consistent with a gut-brain route from microbial community change to neural function.

CoDA via clr-lasso identified *Alloprevotella* as a potential biomarker for EtOH-VEH and *Oscillibacter* for H_2O-VEH (Fig. 9**A**). Biomarkers are ranked by impact, and the associated ROC curve yielded an AUC of 0.741. The Selbal-like plot (Fig. 9**D**) further distinguished groups: *Ruminococcus*, *Enterorhabdus*, *Clostridium_XIVb*, *Escherichia/Shigella*,

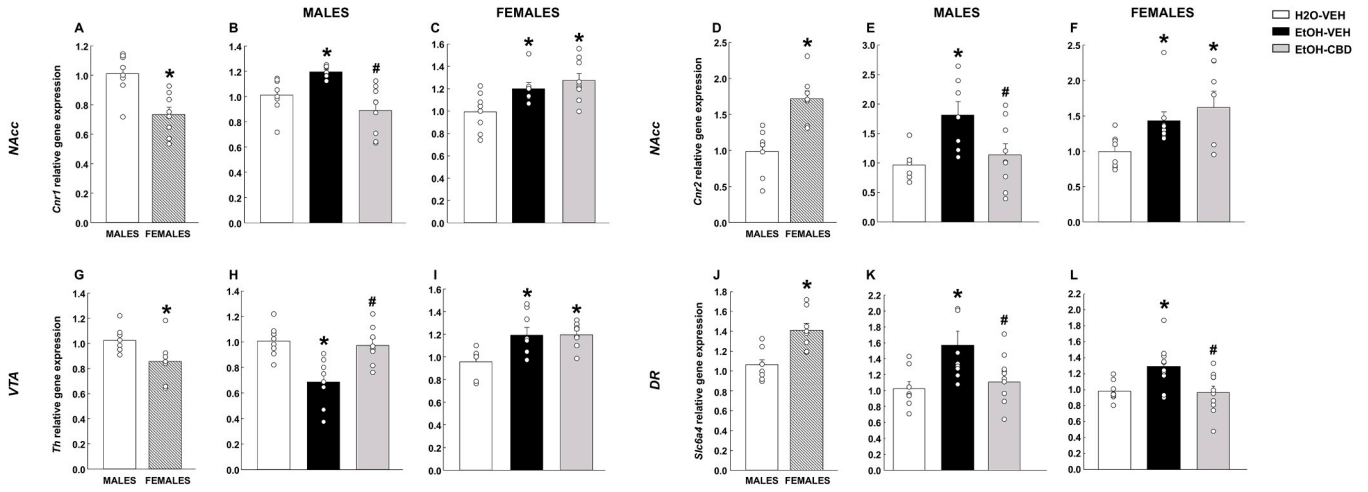

Fig. 4. Real-time PCR analyses in male and female mice perinatally exposed to ethanol and chronically treated with CBD (30 mg/kg/24 h, i.p.). Relative gene expression of cannabinoid receptors 1 (*Cnr1*; A, B, and C; n = 7–9/group) and 2 (*Cnr2*; D, E, and F n = 7–9/group) in the nucleus accumbens (NAcc), tyrosine hydroxylase (*Th*; G, H, and I n = 7–8/group) in the ventral tegmental area (VTA), and 5-hydroxytryptamine transporter (*Slc6a4*; J, K, and L n = 8–10/group) in the dorsal raphe (DR) nucleus was evaluated. * $P < 0.05$ vs H_2O-VEH group; # $P < 0.05$ vs EtOH-VEH group.

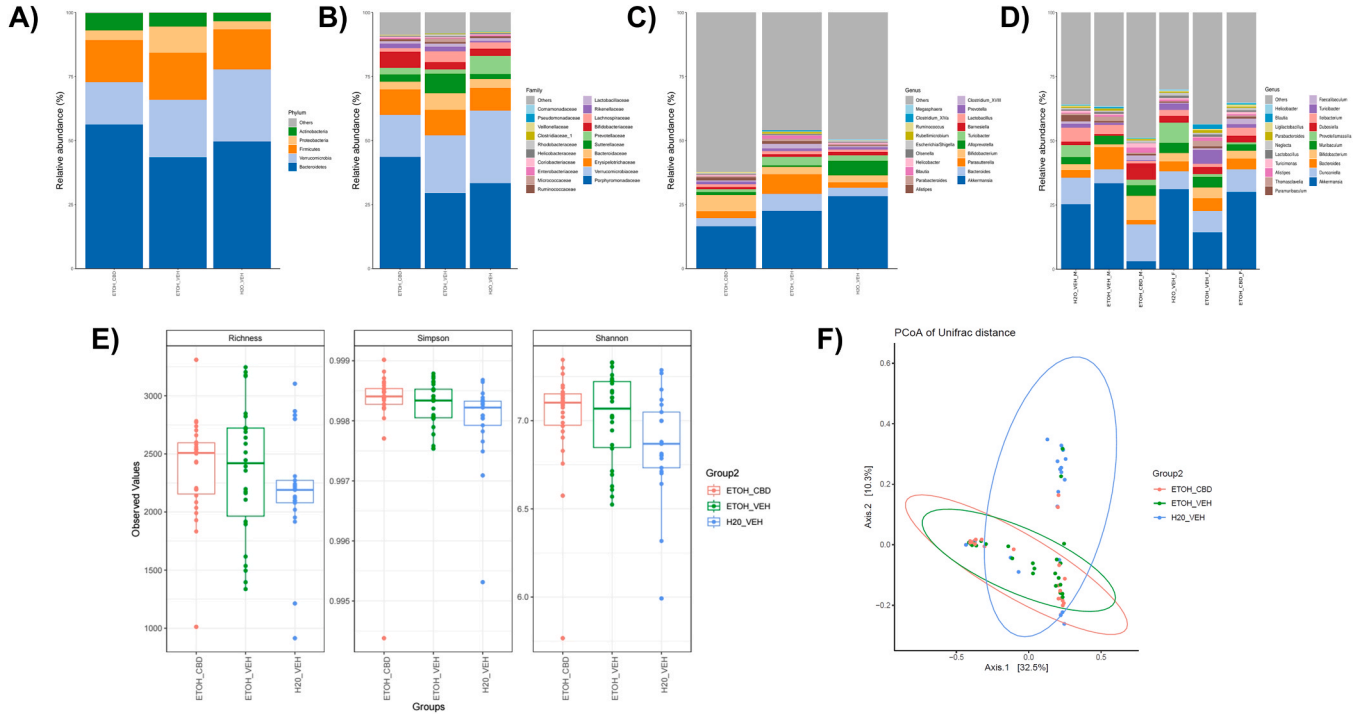

Fig. 5. Gut microbiota composition and diversity across experimental groups (n = 10–12/group). (A-D) Bar plots showing the relative abundance of bacterial taxa at different taxonomic levels: (A) phylum, (B) family, (C) genus, and (D) genus stratified by sex across three treatment groups. (E) Alpha diversity metrics, including richness (observed features), Simpson index, and Shannon index, are presented for each experimental group. (F) Principal Coordinate Analysis (PCoA) based on Bray–Curtis dissimilarity demonstrates significant clustering by treatment group (PERMANOVA, $R^2 = 0.166$, $P = 0.027$).

Mucispirillum, *Pediococcus*, *Faecalibacterium*, and *Intestinomonas* were more abundant in EtOH-VEH, whereas *Prevotella*, *Rubellimicrobium*, *Roseburia*, *Pseudomonas*, *Blastococcus*, *Oscillibacter*, and *Anaerotruncus* were enriched in H_2O-VEH.

3.5.2. Impact of CBD on gut microbiota between EtOH-VEH and EtOH-CBD groups

If we consider the sex of each sample, considerable differences were found (P value < 0.05) in alpha-diversity, both for richness and diversity (Shannon) between EtOH-VEH and EtOH-CBD females, and between EtOH-VEH and EtOH-CBD males. Median alpha diversity tended to be higher in the EtOH-CBD group than in the EtOH-VEH group, although this difference did not reach statistical significance. However, when accounting for sex, significant differences ($P < 0.05$) emerged in both richness and Shannon diversity between EtOH-VEH and EtOH-CBD females, as well as between EtOH-VEH and EtOH-CBD males, highlighting sex-specific effects on gut microbiota diversity (Fig. 6**D**). In beta-diversity (PCoA; Unweighted), a large change between treatments is observed, this being significant as demonstrated by the PERMANOVA test (R2 = 0.20228; P = 0.001). The first component (PCoA1) explains 49 % of the variability of the samples, and the second component (PCoA2) explains 9.5 % (Fig. 6**B**).

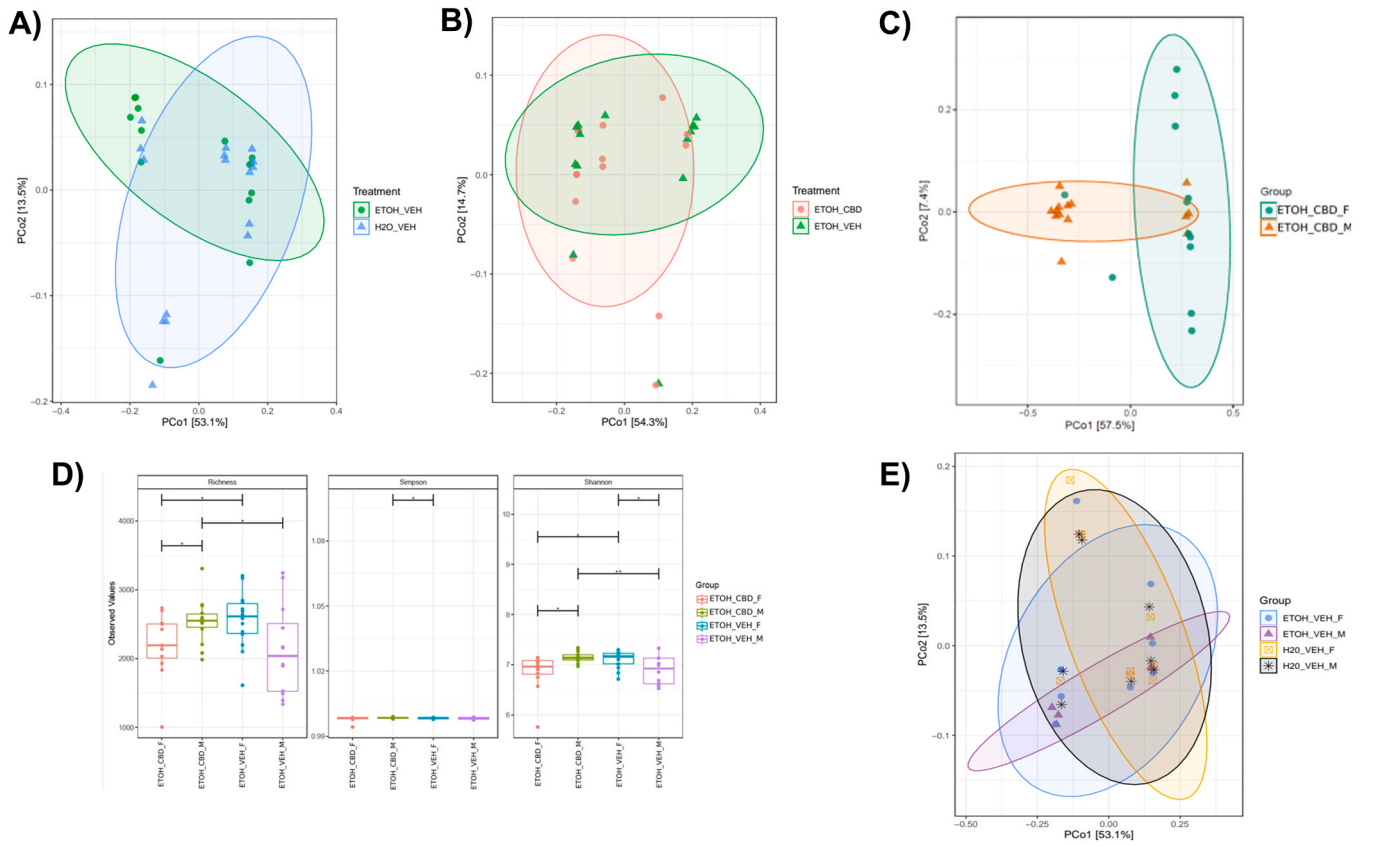

Fig. 6. Beta and alpha diversity analyses of gut microbiota across treatment and sex-stratified experimental groups (n = 10–12/group). (A-C, E) Principal Coordinate Analysis (PCoA) plots based on Bray-Curtis dissimilarity showing clustering of gut microbial communities according to different comparisons: (A) EtOH_VEH vs H_2O_VEH, (B) EtOH_CBD vs EtOH_VEH, (C) EtOH_CBD groups stratified by sex (H: females, M: males), and (E) Sex-stratified groups of EtOH_VEH and H_2O_VEH. (D) Boxplots of alpha diversity indices, including observed richness, Simpson, and Shannon diversity across groups stratified by treatment and sex. Asterisks indicate statistically significant differences (Wilcoxon test, *P < 0.05; **P < 0.01; ***P < 0.001).

In the animal model of FASD, we evaluated the microbiota and the effects of CBD administration on offspring exposed perinatally to ethanol. Analysis of shared zOTUs between the EtOH-VEH and EtOH-CBD groups revealed a core zOTUs overlap of 38.5 %, with 32.4 % being exclusive to the EtOH-CBD group and 29.1 % unique to the EtOH-VEH group (Fig. 7**A**). LEfSe analysis identified significant differences in microbial abundance between the EtOH-VEH and EtOH-CBD groups. Notably, a substantial change of *Alloprevotella* was found in EtOH-CBD, and *Bacteroides*, *Clostridium_XVIII*, *Blautia*, *Escherichia/Shigella*, *Clostridium_XIVa*, *Parabacteroides*, and *Lactobacillus* in EtOH-VEH (Fig. 7**E**).

To assess the influence of behavioral and brain molecular factors on microbial composition between EtOH-VEH and EtOH-CBD groups, the "envfit" function was applied to the Bray-Curtis distance matrix (Fig. 8**D**). This analysis identified significant associations with NA_CB1_Cnr1 ($R^2 = 0.3620$, P = 0.004), FR3 ($R^2 = 0.2417$, P = 0.044), 5HTT ($R^2 = 0.2075$, P = 0.029) and Striatum_cortex_raclopride ($R^2 = 0.2075$, P = 0.051) that were the most relevant factors differentiating between EtOH-VEH and EtOH-CBD groups. Consistent with these associations, the biplot (Fig. 8B) shows that CBD shifted beta-diversity and favored taxa (Alloprevotella, Bifidobacterium, Akkermansia) that aligned with improved emotional performance (higher LDB time) and dopaminergic indices (VTA_TH), whereas EtOH-VEH–enriched genera (Blautia, Clostridium_XVIII, Parasutterella, Bacteroides) aligned with higher DR_Slc6a4 (5HTT), elevated [^{1} ^{1}C]raclopride accumbens/cortex ratios in females, and greater operant motivation (FR/PR). Along RDA1 (11.8 %), EtOH-CBD samples aligned with LDB Time and VTA TH, which was strongly associated with *Allistipes, Alloprevotella* and *Bifidobacterium*. LDB transitions and NA_CB2_Cnr2 were strongly associated with *Akkermansia*. In contrast, *Blautia*, *Turibacter*, *Parasutterella*, *Bacteroides*, *Clostridium_XVIII* and *Rubellimicrobium* were enriched in EtOH-VEH samples, aligning with Cortex_Synaptic_density_11C.UCB.J, Tail_suspension_Test, DR_5HTT, Accumbens_cortex_Raclopride, FR3 and FR1 (Fig. 8**B**). Spearman correlation analysis at the genus level identified a significant positive correlation in *Barseniella* in the Striatum_cortex_raclopride. In the NA_CB1_Cnr1 factor, we observe a significant positive correlation with Akkermansia, Bacteroides, and *Escherichia/Shigella*, and a significant negative correlation with *Ruminococcus* and *Bifidobacterium*. In the *Turibacter* genera, we found a significant positive correlation with the factors Cortex_Synaptic_density_11C.UCB.J, VTA_TH, FR1 and Tail_suspension_Test (Fig. 8**B**).

Differential microbial abundance between EtOH-VEH and EtOH-CBD groups was performed using a compositional data analysis (CoDA) approach, namely clr-lasso. This strategy suggests *that Clostridium XVIII is a possible biomarker in EtOH-CBD and Helicobacter is* a potential biomarker in EtOH-VEH (Fig. 9**B**). Potential biomarkers distinguishing EtOH-VEH and EtOH-CBD are displayed, ranked from the most to the least significant, together with a ROC curve (AUC = 0.747) and density distributions for each group. The Selbal-like plot (Fig. 9**E**) highlights the keystone taxa associated with each condition: *Ruminococcus, Bifidobacterium, Clostridium XVIII,* and *Parabacteroides* with EtOH-CBD samples, whereas *Escherichia/Shigella, Mucispirillum, Pseudomonas, Helicobacter,* and *Deinococcus* are linked to EtOH-VEH samples.

CBD-shifted communities (e.g., Alloprevotella, Bifidobacterium, Akkermansia) aligned with improved LDB performance and dopaminergic indices (VTA_TH), compatible with enhanced epithelial integrity, reduced pro-inflammatory signaling, and restoration of gut–brain homeostasis.

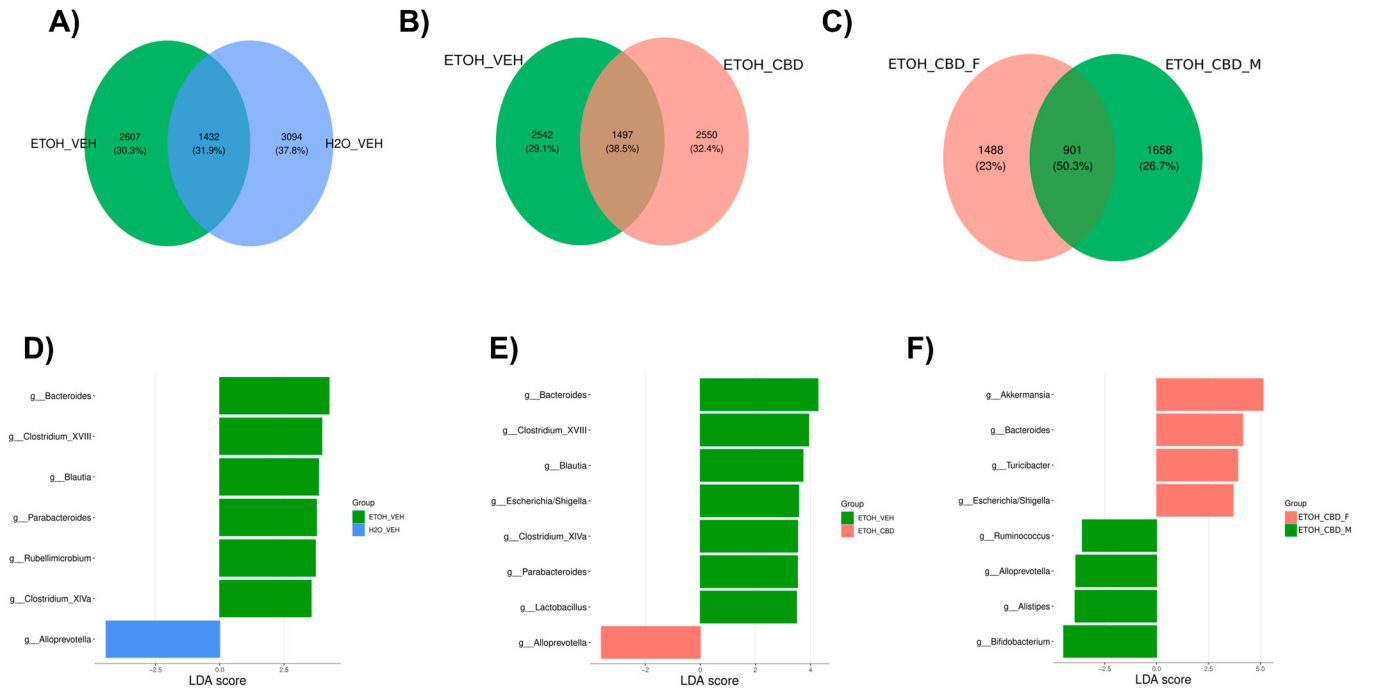

Fig. 7. Core microbiota overlap and differential taxonomic signatures across experimental groups (n = 10–12/group). (A-C) Venn diagrams showing shared and unique amplicon sequence variants (ASVs) between groups: (A) EtOH_VEH vs H_2O_VEH, (B) EtOH_CBD vs EtOH_VEH, and (C) EtOH_CBD_F (females) vs EtOH_CBD_M (males). (D-F) Linear discriminant analysis effect size (LEfSe) plots showing differentially abundant bacterial genera between: (D) EtOH_VEH and H_2O_VEH, (E) EtOH_CBD and EtOH_VEH, and (F) EtOH_CBD_H and EtOH_CBD_M.

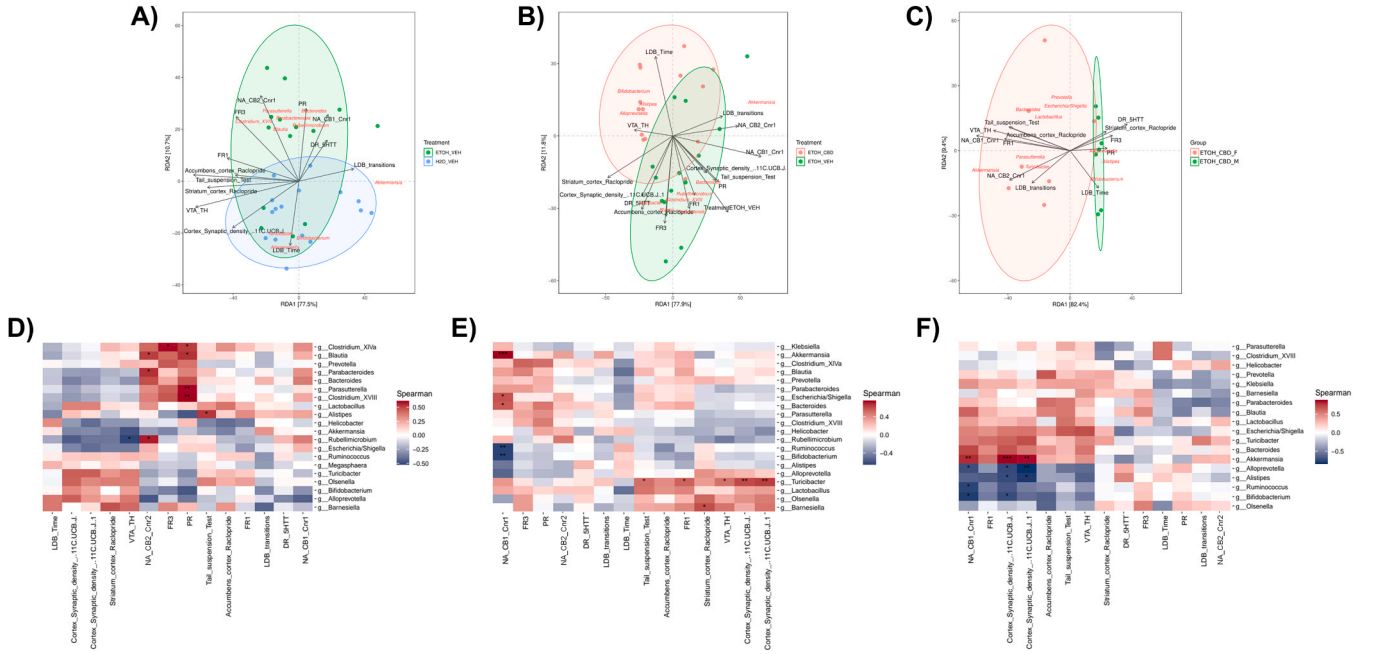

Fig. 8. Associations between gut microbiota composition and behavioral/neurochemical outcomes across treatment groups (n = 10–12/group). (A-C) Redundancy analysis (RDA) biplots illustrating the relationships between microbial genera (red text) and behavioral/neurochemical variables (black vectors) in: (A) EtOH_VEH vs H_2O_VEH, (B) EtOH_CBD vs EtOH_VEH, (C) EtOH_CBD_H vs EtOH_CBD_M. (D-F) Heatmaps showing Spearman correlation coefficients between significantly abundant bacterial genera and behavioral/neurochemical variables for the same group comparisons as in A-C. Asterisks denote significance (*P < 0.05, **P < 0.01).

3.5.3. Distinct impact of CBD on gut microbiota of EtOH-exposed mice depending on sex

Alpha diversity analysis showed significant sex-related differences in richness and diversity (Shannon index), with EtOH-CBD females and males groups displaying distinct microbial profiles (Fig. 6**D**). Beta diversity analysis (PCoA; unweighted) confirmed significant differences between sexes (R^2 = 0.21548; P = 0.001), with the first two principal components explaining 57.5 % and 9.5 % of the variance, respectively (Fig. 6**C**). Interestingly, no significant sex-based differences were found within the EtOH-VEH group; however, sex significantly influenced microbial composition in the EtOH-CBD group.

Shared zOTU analysis between EtOH-CBD females and males groups

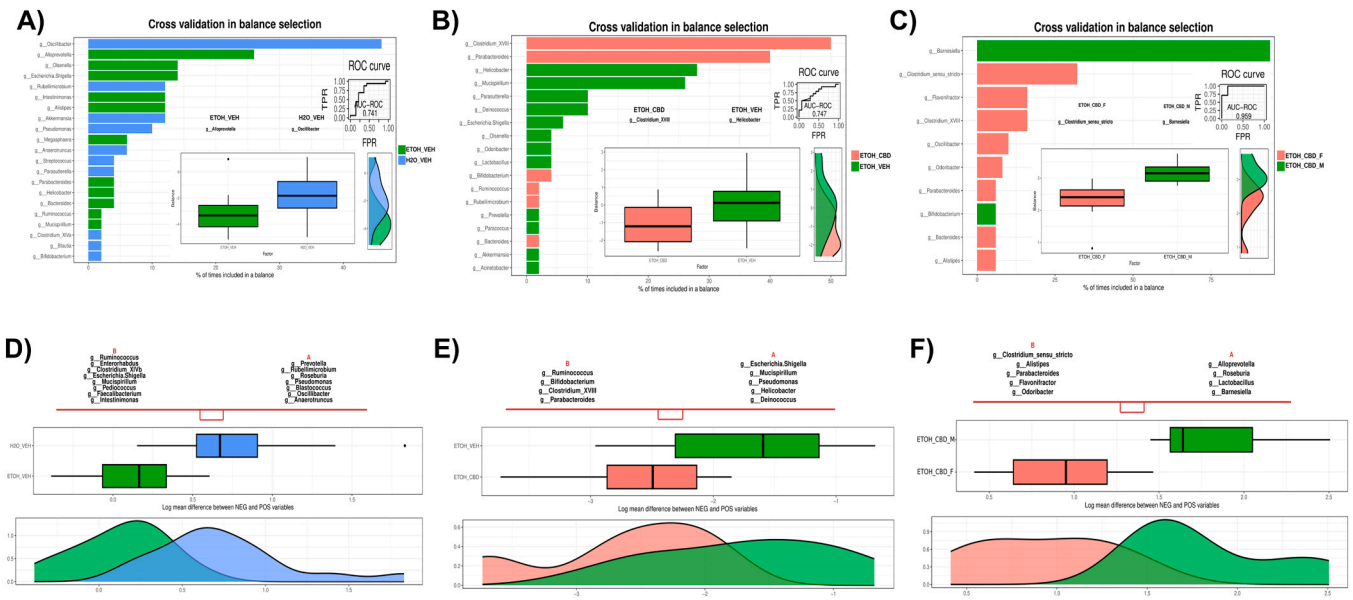

Fig. 9. Differential microbial signatures and balances across experimental groups, as assessed using SELBAL and CLR-LASSO models (n = 10–12/group). (A-C) Barplots represent microbial genera most frequently included in balance selection (via cross-validation) that discriminate between: (A) H_2O_VEH vs EtOH_VEH, (B) EtOH_CBD vs EtOH_VEH, and (C) EtOH_CBD_H vs EtOH_CBD_M. Boxplots below each barplot indicate the distribution of balance scores by group, and adjacent ROC curves reflect classification performance. (D-G) CLR-LASSO models showing log-ratio differences between groups for the same pairwise comparisons. Boxplots indicate the magnitude of the CLR-transformed differences, with density plots below representing the distribution of effect sizes. Microbial genera contributing positively or negatively to the model are annotated above each plot.

revealed a 50.3 % core overlap, with 23 % of zOTUs unique to females and 26.7 % exclusive to males (Fig. 7**A**). LEfSe analysis identified key sex-associated taxa: *Bifidobacterium*, *Alistipes*, *Alloprevotella*, and *Ruminococcus* were enriched in males, whereas *Akkermansia*, *Bacteroides*, *Turicibacter*, and *Escherichia/Shigella* were more abundant in females (Fig. 7**F**).

RDA using the Bray-Curtis matrix and "envfit" function identified several variables significantly associated with microbial composition: NA_CB1_Cnr1 (R^2 = 0.6614, P = 0.003), NA_CB2_Cnr2 (R^2 = 0.4231, P = 0.003), FR3 (R^2 = 0.1983, P = 0.007), DR_5HTT (R^2 = 0.2305, P = 0.001), LDB_Time (R^2 = 0.1473, P = 0.044), VTA_TH (R^2 = 0.4872, P = 0.041), Cortex_Synaptic_Density ([11 C]UCB-J) (R^2 = 0.7625, P = 0.002), and Accumbens_Cortex_Raclopride (R^2 = 0.1425, P = 0.049) (Fig. 8**F**). RDA1 (82.4 %) indicated that EtOH-CBD male samples aligned with LDB Time, PR, FR3, Striatum_Cortex_Raclopride, and DR_5HTT, and were associated with *Alistipes*, *Alloprevotella*, and *Bifidobacterium*. In contrast, EtOH-CBD female samples aligned with NA_CB2_Cnr2, FR1, VTA_TH, NA_CB1_Cnr1, LDB transitions, and Accumbens_Cortex_Raclopride, and were enriched in *Akkermansia*, *Turicibacter*, *Parasutterella*, *Bacteroides*, *Lactobacillus*, *Prevotella*, and *Escherichia/Shigella* (Fig. 8**C**). Spearman correlation analysis showed *that Akkermansia was positively correlated with NA_CB1_Cnr1 and Cortex_Synaptic_Density, whereas Alloprevotella, Alistipes, Ruminococcus, and Bifidobacterium showed significant negative correlations with these* factors (Fig. 8**F**).

Sex moderated the CBD → microbiota → brain/behavior linkage: in males, CBD-enriched Alloprevotella/Bifidobacterium/Alistipes aligned with higher LDB time and lower DR_Slc6a4 (5HTT), whereas in females, Akkermansia/Turicibacter enrichment aligned with NA_CB1/Cnr1 and cortical [^{1} ^{1}C]UCB-J, paralleling CBD's normalization of female-biased ethanol motivation (FR/PR). Differential abundance analysis using clr-lasso (CoDA approach) identified *Barnesiella* as a potential male biomarker and Clostridium *sensu stricto* as a possible female biomarker (Fig. 9**C**). The corresponding ROC curve had an AUC of 0.959. A Selbal-like plot (Fig. 9**F**) highlighted sex-specific genera: *Clostridium sensu stricto*, *Alistipes*, *Parabacteroides*, *Flavonifractor*, and *Odoribacter* were enriched in females, whereas *Alloprevotella*, *Roseburia*, *Lactobacillus*, and *Barnesiella* were predominant in males. This sex contingency matches known hormone-ECS-microbiota cross-talk and supports the view that the microbiota acts as a mechanistic hub for sex-dependent outcomes.

3.6. *Sex-dependent effects of PAE on oral ethanol self-administration (OEA) and CBD-mediated reduction of the motivation to consume alcohol*

In male mice, no differences were detected between mice exposed to the FASD model and treated with the VEH or CBD and controls in the number of effective responses (Fig. 10**A**; One-way RM ANOVA, FR1, Treatment F [2,179] = 2.488 P = 0.100, Day F [4,179] = 3.843 P = 0.006, Treatment x Day F [8,179] = 1.043 P = 0.408; FR3, Treatment F [2,179] = 1.376 P = 0.268, Day F [4,179] = 1.735 P = 0.147, Treatment x Day F [8,179] = 1.918 P = 0.063) nor the ethanol intake (Fig. 10**B**; One-way RM ANOVA, FR1, Treatment F [2, 179] = 1.981 P = 0.156, Day F [4,179] = 17.543 P < 0.001, Treatment x Day F [8,179] = 1.361 P = 0.221; FR3, Treatment F [2,179] = 0.443 P = 0.646, Day F [4,179] = 4.232 P = 0.003, Treatment x Day F [8,179] = 0.543 P = 0.822) in both FR1 and FR3 stages of the OEA paradigm. In females, animals exposed to the FASD model showed a higher number of effective responses (Fig. 10**C**; One-way RM ANOVA, FR1, Treatment F [2,179] = 5.285 P = 0.010, Day F [4,179] = 8.795 P < 0.001, Treatment x Day F [8,179] = 1.082 P = 0.380; FR3, Treatment F [2,179] = 4.315 P = 0.022, Day F [4,179] = 0.832 P = 0.507, Treatment x Day F [8,179] = 2.022 P = 0.049) and ethanol intake (Fig. 10**D**; One-way RM ANOVA, FR1, Treatment F [2, 179] = 9.769 P < 0.001, Day F [4,179] = 4.174 P = 0.003, Treatment x Day F [8,179] = 1.544 P = 0.148; FR3, Treatment F [2,179] = 5.243 P = 0.011, Day F [4,179] = 9.848 P < 0.001, Treatment x Day F [8,179] = 0.656 P = 0.729) in FR1 and FR3 of the OEA paradigm, which was normalized with CBD administration.

In the progressive ratio stage of the OEA paradigm, no differences were found between all three groups of male mice in the breaking point (Fig. 10**E**; One-way ANOVA, F [2,35] = 0.268, P = 0.766) nor in the ethanol intake (Fig. 10**F**; One-way ANOVA, F [2,35] = 0.024, P = 0.976) evaluation. Interestingly, in the female group, a statistically significant increase was identified in breaking point (Fig. 10**G**; One-way ANOVA, F

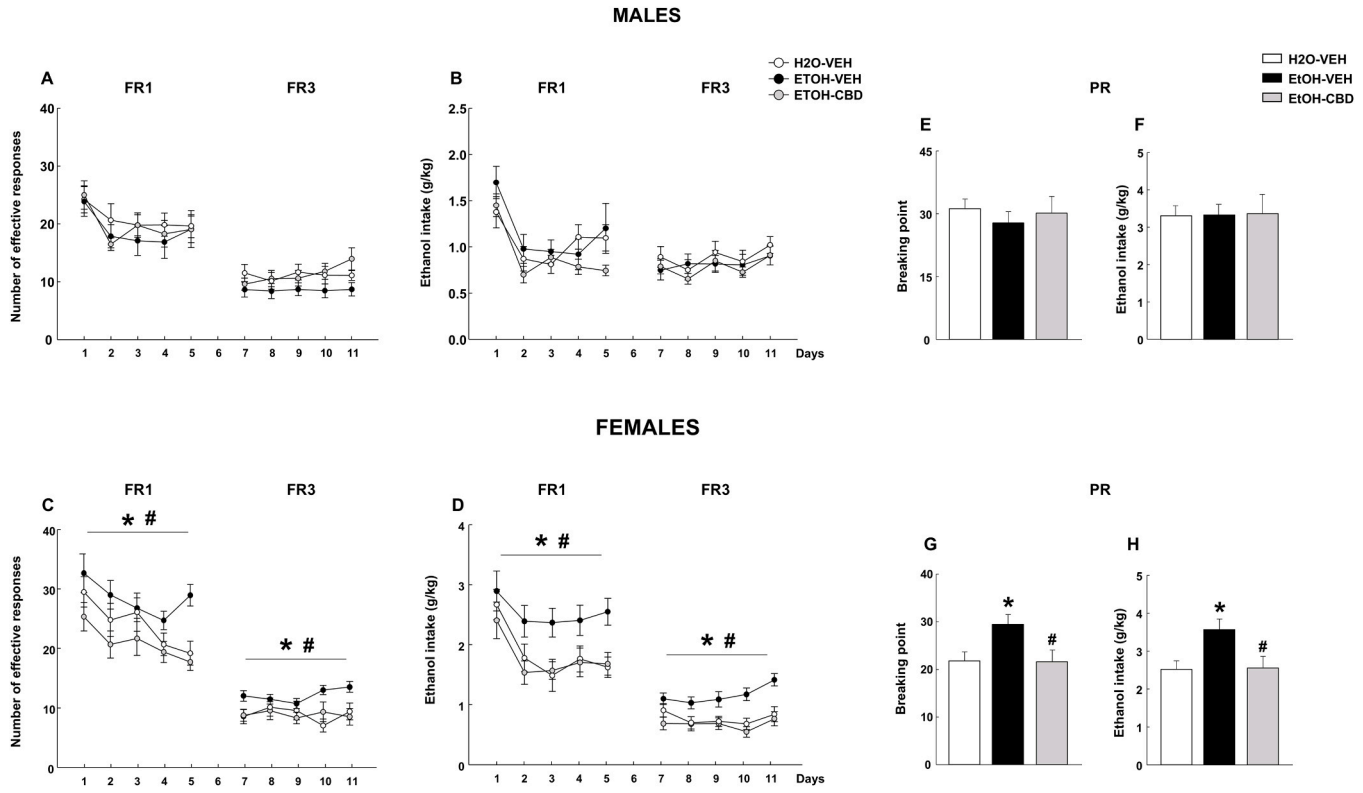

Fig. 10. Evaluation of the effects of CBD (30 mg/kg/24 h, i.p.) on ethanol oral self-administration in male and female mice perinatally exposed to ethanol. (A, C) Number of effective responses during the fixed ratio 1 (FR1) and fixed ratio 3 (FR3) phases (n = 10–14/group); (B, D) ethanol intake expressed as g/kg during the FR1 and FR3 phases (n = 10–14/group); (E, G) breaking point achieved during progressive ratio (PR) (n = 10–14/group); and (F, H) ethanol intake expressed as g/kg during PR (n = 10–14/group). The dots and the columns represent the means and vertical lines ± the standard error of the mean (SEM). * $P < 0.05$ vs H_2O-VEH group; # $P < 0.05$ vs EtOH-VEH group.

[2,35] = 4.709, P = 0.016) and ethanol intake (Fig. 10**H**; One-way ANOVA, F [2,35] = 5.094, P = 0.012), and both of them were normalized with the early and chronic administration of CBD.

3.7. *Integrated microbiota-brain-behavior analysis*

To make explicit the connections among domains, we summarized cross-domain effects using constrained ordination and targeted associations. Across groups, RDA/envfit consistently linked community structure to ECS (Cnr1/Cnr2), monoaminergic (Th, Slc6a4), synaptic ([^{11}C]UCB-J), and motivational (FR1/FR3/PR) variables (Fig. 8A–F). Genera enriched by PAE (e.g., Bacteroides, Blautia, Clostridium_XIVa, Clostridium_XVIII, Parasutterella) were associated with higher depressive-like behavior (TST) and greater ethanol motivation (PR, FR3). In contrast, genera favored by CBD (e.g., Alloprevotella, Bifidobacterium, Akkermansia) tracked with improved emotional performance (LDB) and dopaminergic normalization (VTA_TH, [^{11}C] raclopride ratios). These multivariate patterns were sex-dependent, paralleling the female-specific elevations in ethanol motivation and their normalization with CBD. Associations were evaluated with multiple-testing control where applicable (FDR), and the direction of arrows/loadings in biplots was interpreted in conjunction with univariate correlations (Fig. 8B–C, F) and CoDA-based feature selection (Fig. 9). Importantly, these results are correlational and do not imply causality. Mechanistically, our data support a testable framework in which PAE-induced dysbiosis and impaired barrier function increase peripheral immune signaling (e.g., LPS–TLR4) and alter microbial metabolite pools (e.g., SCFAs, indoles acting on AhR), thereby modulating ECS and monoaminergic pathways that converge on the observed behavioral and motivational phenotypes. CBD would act both peripherally—by improving barrier integrity and reshaping microbial ecology—and centrally—by normalizing ECS/5-HT readouts—closing the gut–brain loop.

4. Discussion

This study provides data on the sex-dependent emotional and molecular alterations induced by PAE in the offspring, highlighting the critical role of gut microbiota, which likely underlie the differential vulnerability to alcohol consumption and motivation between male and female mice in the OEA paradigm. Notably, early (PND21) and chronic (5–10 weeks) treatment with CBD showed a very significant improvement and/or modulatory effect. The following statements support the main findings of this study: 1) Male and female mice exposed to the animal model of FASD showed increased anxiety- and depressive-like behavior that was normalized with CBD treatment; 2) Autoradiographic studies revealed sex-dependent changes in synaptic density and D2/D3 receptors availability associated with PAE; 3) *Cnr1/Cnr2*, *Th*, and *Slc6a4* gene expression was sex-dependently altered in the NAcc, VTA, and DR of mice exposed perinatally to ethanol, respectively, and CBD normalized these alterations particularly in male subjects; 4) PAE caused sex-differentiated gut microbiota dysbiosis, reflected in greater alpha variability and clustering in beta diversity analysis; 5) The administration of CBD in animals exposed to the FASD model improved microbial diversity, promoted a clear separation in beta diversity compared to the VEH-treated group exposed to the FASD model, and enriched protective bacterial species; and 6) Female but not male offspring exposed to ethanol during gestation and lactation showed a higher motivation to drink ethanol, and CBD produced a complete normalization. We emphasize that cross-domain associations reported here are correlational and should not be interpreted as evidence of causality

A previous study in our laboratory revealed that PAE in C57BL/6 J

male and female mice induced significant behavioral alterations reflecting increased anxiety- and depressive-like behavior, cognitive disturbances, and enhanced reactivity (startling response) [27]. In agreement with those findings, we replicated here the emotional deficits, as well as the anxiolytic and antidepressant effects of CBD. These findings allow us to confirm not only the reproducibility of our animal model of FASD but also the therapeutic potential of CBD for the management of the mood disorders encompassing this clinical condition. After the behavioral evaluation, the animals were sacrificed five weeks after weaning and the start of the CBD or VEH treatment to analyze changes in specific biomarkers from brain and fecal samples using different technical approaches. We interpret the cross-domain consistencies (behavioral, molecular, microbial) as convergent evidence, while avoiding causal language.

In vitro autoradiography experiments revealed a significant reduction of synaptic density (measured by [^{11}C]UCB-J) only in the cortex and HIPP of males, which CBD slightly improved, whereas no changes were observed in females. In this regard, one of the earliest studies reported decreased synaptic density in the frontal cortex of neonatal rats exposed to ethanol in utero [69], without differentiating between male and female rats. However, the accumulating evidence suggests that PAE induces sex-dependent effects on hippocampal synaptic plasticity. Indeed, PAE has been shown to reduce hippocampal cell survival in male offspring [70] but not in females [71]. In addition, PAE has been associated with reduced hippocampal long-term potentiation (LTP), which is involved in learning and memory processes, in the CA1 or dentate gyrus (DG) subregions of the HIPP in males, whereas inducing no changes or even a facilitation effect in females [72–74]. However, a recent study found that PAE similarly affects male and female mice's hippocampal neuronal arborization, evaluating branching complexity and dendritic length [75]. This opposite effect in the case of females could be due to essential differences in the animal model employed to simulate FASD, namely the administration of a higher ethanol dosage (5 g/kg vs. 3 g/kg), through a different route of administration (i.p. vs. p.o.), and at a different time point (from PND2 to PND8 directly to pups vs. from GD5 to PND21 to mothers). Thus, while our male-specific SV2A reductions align with parts of the literature, we refrain from inferring a mechanism from these associations alone.

According to previous reports, PAE heightens dopaminergic activity in the VTA and alters postnatal ethanol-induced dopaminergic activity in brain areas of the mesolimbic reward circuit, including the NAcc [76]. Still, the precise molecular mechanisms underlying the sex specific differences are poorly understood. In this study, we show a reduction in the striatum/cortex ratio of males' dopamine D2/D3 receptor availability. This result is in line with a previous report using [3 H]raclopride, which showed a significantly decreased number of dopamine D2 binding sites in the dorsal and ventral striatum. Interestingly, only in those animals perinatally exposed (GD8 to GD20) to 3 g/kg/day of ethanol, without finding differences in the 5 g/kg/day group [77]. On the contrary, D2/D3 receptor availability was higher in females, especially when considering the accumbens/cortex ratio. In an animal model of gestational ethanol exposure in C57BL/6 J mice, the authors report increased stimulus-evoked dopamine levels in the dorsolateral striatum only in female mice, suggesting a relevant sex-dependent effect on the striatal dopaminergic activity [78]. We present these dopaminergic and behavioral co-variations cautiously, recognizing that mediation has not been demonstrated.

The relative gene expression analyses were focused on evaluating changes in concrete targets that could be related, at least in part, with the emotional disturbances in the offspring exposed to the FASD animal model (*Slc6a4* in the DR), the pharmacological treatment with CBD (*Cnr1* and *Cnr2* in the NAcc), or the vulnerability to alcohol consumption and motivation in the OEA (*Th* in the VTA).

Depression is associated with alterations in the expression, availability and/or function of the serotonin transporter, the main target of antidepressant drugs [79]. Although several reports have linked depressive behavior with reduced levels of the serotonin transporter, some studies have shown increased DR expression of the *Slc6a4* gene in rodent models of exercise cessation [80] and post-traumatic stress disorder (PTSD) [81] associated with depressive-like states, as well as an enhanced functional state in patients during depressive episodes [82]. Accordingly, in our study, *Slc6a4* gene expression was upregulated in females under basal conditions (H_2O-VEH groups), who exhibited longer immobility times in the TST than males, as well as in EtOH-VEH groups from both sexes, which also showed increased behavioral despair. Interestingly, the antidepressant effects of CBD were accompanied by the normalization of Slc6a4 gene expression in the DR of male and female animals. Slc6a4 normalization might be an associated signature of CBD's behavioral effects, not as proof that 5-HTT mediates those effects.

The endocannabinoid system (ECS) has been closely involved in the alterations induced by PAE [10,11]. Indeed, we showed significant alterations in the gene expression of *Cnr1* and *Cnr2* in the HIPP of mice exposed to the FASD animal model, which were normalized by CBD only in males, but not in females [27]. The present work focused on the NAcc due to its role in drug addiction and the evaluation of the PAE-induced vulnerability to alcohol rewarding and motivational actions. Both cannabinoid receptors were significantly upregulated in those animals perinatally exposed to alcohol, but CBD normalizes this effect only in males. Further studies are needed to clarify sex-dependent differences in the molecular alterations induced by PAE in the ECS, as well as the effects of CBD.

On the other hand, the exposure to alcohol during gestation and lactation induced opposite sex-associated changes in the gene expression of *Th*, the rate-limiting enzyme of dopamine synthesis, measured in the VTA. While a reduction was found in males, the *Th* gene expression was upregulated in females, a result that resembles the changes in striatal dopaminergic D2/D3 receptor availability observed in autoradiographic studies. These results suggest that the differences in dopaminergic targets in the mesolimbic reward system might underlie the pronounced disparities in alcohol motivation between males and females. A previous report indicated that PAE leads to a persistent increase in excitatory synaptic strength in VTA dopaminergic neurons, contributing to enhanced sensitivity to drugs of abuse and increased addiction risk. This effect may be mediated by a potentiation of endocannabinoid signaling [4]. Thus, future investigations are needed to delve deeper into the role of these mechanisms in PAE-induced alcohol addiction and CBD-mediated improvement effects from a sex perspective.

Microbiota and sex hormones influence each other, including via the intestinal "estrobolome"; such bidirectional regulation can shape systemic steroid milieu and neural function [41]. Given the female-biased ethanol motivation, a hormone–microbiota interface is a plausible, testable route in our model, although we did not assay sex-steroid pathways. Mechanistic context (hypothesis; microglia/immune). Microbiota regulate microglial maturation and immune tone, offering a pathway from dysbiosis to synaptic/monoaminergic alterations. This remains speculative here and requires interventional designs (e.g., microbiota depletion/reconstitution) with microglial and cytokine endpoints.

Microbial short-chain fatty acids can modulate histone deacetylase activity and neuroimmune signaling, suggesting an epigenetic conduit from community shifts to ECS/monoaminergic endpoints. We did not quantify SCFAs or chromatin marks, so this remains a testable hypothesis.

Alpha- and beta-diversity indicated that prenatal ethanol (PAE) altered gut composition and increased within-group variability, consistent with gestational alcohol studies [37,83]. PAE enriched putatively pro-inflammatory genera (e.g., *Bacteroides, Clostridium_XVIII, Blautia, Rubellimicrobium*) and reduced taxa often considered beneficial (*Bifidobacterium, Alloprevotella*), with sex-dependent differences (male-biased Bacteroides/Bifidobacterium; female-specific shifts such as *Faecalitalea/Proteus*) [84]. Exposure typically lowered richness/evenness and expanded Proteobacteria/Actinobacteria while reducing

SCFA-producing groups (*Ruminococcus, Lachnospiraceae*) [85]. Notably, Alistipes increased and correlated with depressive-like behavior (TST), aligning with links to alcoholism, depression, and inflammation [86]. Prior work shows prenatal alcohol/maternal stress can produce enduring microbiota changes and metabolite shifts (e.g., phenols, indoles) in maternal–fetal compartments [87]. Collectively, the dysbiosis observed may promote LPS–TLR4 signaling and neuroinflammation in FASD [34]. We stress that these alignments support plausibility but do not substitute for causal tests.

Taken together, our integrative analyses support a coherent pathway whereby PAE induces an alteration shift (enrichment of *Bacteroides, Blautia, Clostridium_XIVa, Clostridium_XVIII and Parasutterella*), which aligns with ECS (Cnr1/Cnr2) and monoaminergic alterations (Slc6a4; sex-divergent Th and D2/D3 availability) and with increased anxiety/depressive-like behavior and ethanol motivation, predominantly in females. CBD partially reverses this cascade by enriching taxa linked to epithelial integrity and anti-inflammatory tone (*Alloprevotella, Bifidobacterium, Akkermansia*), concomitant with normalization of brain markers and behavior/motivation. To move from association to mechanism, future work should deploy sex-stratified fecal microbiota transfer (FMT), antibiotic depletion/rescue, targeted augmentation of candidate taxa, and formal mediation analyses linking microbial features, ECS/monoaminergic readouts, and behavior [88]. While causality cannot be inferred, the concordance across microbiota, brain, and behavioral domains, and the sex-specificity of these links, strengthen the interpretation that the gut–brain axis contributes to PAE sequelae and to CBD's benefits [41].

Microbiota-centered mechanistic interpretation. Our data support a model in which PAE precipitates a dysbiotic shift (*Bacteroides, Blautia, Clostridium_XIVa/XVIII, Parasutterella*) compatible with reduced ecological stability and barrier compromise; through LPS-TLR4 signaling and shifts in short-chain fatty acids and indole derivatives (AhR), peripheral cues reshape ECS (Cnr1/Cnr2), serotonin transporter expression (Slc6a4), and dopaminergic tone (sex-divergent Th and D2/D3 availability), converging on anxiety-/depressive-like behavior and ethanol motivation [41]. CBD enriches taxa linked to mucosal homeostasis and anti-inflammatory metabolism (*Alloprevotella, Bifidobacterium, Akkermansia*) and concomitantly normalizes neural and behavioral endpoints along this gut–brain axis [41]. CBD increased microbial diversity and shifted community structure, enriching Alloprevotella, Bifidobacterium, and Akkermansia— the latter linked to mucosal integrity and anti-inflammatory tone [89]. Evidence from other models shows CBD can restore microbial balance and reduce hyperpermeability (sometimes alongside fish oil) [90], while cannabinoids support barrier and immunomodulation via FAAH and CB1/CB2 pathways. Bidirectional microbiota–ECS influences may further contribute, and CBD has been reported to modulate immune responses and intestinal permeability [91]. In our dataset, CoDA highlighted Clostridium_XVIII and Oscillibacter as discriminative taxa between EtOH-VEH and EtOH-CBD, suggesting targeted shifts relevant to intestinal homeostasis. Again, these taxonomic shifts co-vary with neural and behavioral readouts, but causality awaits interventional proof.

A novel finding is the evident sex dimorphism in the microbial response to CBD. In males, CBD-enriched Bifidobacterium, Alistipes, and Alloprevotella, whereas in females, Akkermansia, Turicibacter, and Escherichia/Shigella predominated; the prominence of Turicibacter in females is notable given its roles in lipid metabolism, inflammation, and permeability [92]. This pattern is plausibly influenced by hormonal modulation of the ECS [93]. It mirrors prior reports of sex-dependent neurobiological and behavioral effects of prenatal ethanol and treatments [39], with similar sex-specific microbial signatures seen in metabolic/neuropsychiatric contexts [94]. We therefore propose sex hormones, immune–microglial tone, and epigenetic regulation as parallel hypotheses for future testing. Correlation analyses linked several genera with neurobiological readouts (CB1/CB2, synaptic density, behavior). Notably, *Rubellimicrobium* correlated positively with Cnr2, whereas *Bifidobacterium* correlated negatively with neuroinflammation markers, consistent with metabolite-mediated (SCFAs, tryptophan) effects on neural signaling [88]. Prior research shows that the microbiota can drive depressive-like behavior via ECS modulation [95], suggesting that CBD effects may involve a dual pathway: direct neuronal receptor actions and microbiota remodeling, in line with FASD models invoking dysbiosis, barrier permeability, and microglial activation. Nevertheless, we refrain from causal claims and outline interventional tests above to adjudicate among mechanisms. Preclinical animal models of FASD have revealed a higher predisposition to the stimulant, reinforcing and motivational actions of ethanol in neonatal [96], adolescent [5,97,98] or adult [99] life periods. However, the differences in vulnerability to the reinforcing effects of alcohol between males and females who were exposed to this drug during the perinatal period are still largely unknown. Females may be more vulnerable to alcohol abuse due to enhanced rewarding effects mediated by the presence of ovarian hormones [100]. In this sense, PAE increased female, and not male, sensitivity to the stimulant effects of ethanol [99]. Likewise, a recent study evaluated the impact of PAE on alcohol operant self-administration in adulthood, showing a similar result in terms of no changes in males and an increase in the number of responses and alcohol intake in females [6]. Accordingly, our study demonstrates that the increase in motivation to consume alcohol induced by PAE varies by sex. There was a clear and significant increase in the number of effective responses, alcohol intake, and cut-off point in females, while there was no change in males. These results highlight sex-dependent differential vulnerability and suggest that females are more predisposed to developing alcohol addiction in the context of FASD. Importantly, early and chronic intervention with CBD normalizes alcohol consumption and motivation completely, pointing out this pharmacological approach as a promising intervention to treat FASD-induced alcohol addiction, particularly in females. Future work should test whether microbiota modulation contributes causally to this female-specific normalization.

A significant strength of this work is the use of a voluntary PAE model, incorporating both pre-gestational drinking and oral ethanol administration throughout gestation and lactation, which closely mimics clinical patterns of PAE and enhances translational relevance. The multidimensional approach, combining behavioral testing, molecular neurobiology (autoradiography and gene expression), and microbiota profiling, also provides a comprehensive view of CBD's therapeutic effects [101], with consistent inclusion of sex as a biological variable. However, while this study offers an integrative approach to the FASD-microbiota-CBD relationship, it has limitations. For instance, the use of a murine model requires caution when extrapolating to humans. Additionally, the current design identifies correlations but cannot prove causality. We therefore reframe mechanistic statements as hypotheses and outline concrete experiments to test them. Future studies should implement direct microbiota interventions, such as fecal transplantation (FMT) or targeted dietary modulation, to confirm the mediating role of the identified taxa.

Furthermore, the study used a single CBD dose and administration route, without dose-response or route comparison, which may limit translational applicability. Microbial function was not assessed (e.g., metabolomics, SCFA profiling), nor was deep sequencing (for functional pathways and species- and strain-level resolution), and outcomes were evaluated at a single post-treatment time point, limiting insight into the long-term stability of effects. Finally, while potential microbial and molecular biomarkers were identified, they require validation in independent cohorts or human studies. Incorporating functional analyses (metabolomics, metagenomics and transcriptomics) will allow characterization of the metabolites involved and their signaling pathways within the gut-brain axis. Given the evidence of sexual dimorphism, future trials should stratify by sex and consider hormonal phases in females, as well as explore potential synergies between CBD and other probiotic, prebiotic or biotic strategies. Prospective, pre-registered, sex-stratified designs will be essential to address causality and

reproducibility.

5. Conclusions

Together, our findings reveal that PAE profoundly alters gut microbiota and that CBD can modulate this dysbiosis, promoting beneficial taxa and modifying community structure in a sex-dependent manner. CBD administration also mitigated anxiety- and depression-like behaviors and modulated gene expression of endocannabinoid and monoaminergic markers. The associations found between microbiota and neurobiological parameters reinforce the idea that the gut microbiota is not a passive actor but an active component in FASD pathophysiology. Consistently, the microbiota shifts we observed co-varied with core brain readouts, including ECS markers (Cnr1/Cnr2), monoaminergic indices (Th, Slc6a4), and imaging-derived measures ([^{11}C]UCB-J and [^{11}C]raclopride ratios) and are consistent with, but do not establish, causal links along the gut-brain axis. Importantly, by integrating constrained ordination and targeted associations, we show that microbiota shifts co-vary with brain readouts and behavioral/motivational phenotypes, outlining a plausible PAE-microbiota-brain-behavior pathway that is modulated by CBD, especially in females. Mechanistic explanations for the observed sex differences remain provisional; hormonal, immune-microglial, and epigenetic routes are promising but require direct testing. This study opens the door to the development of personalized interventions aimed at restoring the microbiota and modulating the gut-brain axis to mitigate the cognitive and behavioral deficits characteristic of this disorder. Future research should use causal designs (e.g., sex-stratified fecal microbiota transfer, targeted microbial augmentation/deletion, cannabinoid receptor modulation, and longitudinal multi-omics) to validate these hypotheses and assess the durability of effects across multiple time points. While causality remains to be established, the quantitative co-variation across domains provides a testable framework for CBD's microbiota-centered mechanism in PAE.

CRediT authorship contribution statement

F. Navarrete: Writing – review & editing, Writing – original draft, Visualization, Validation, Supervision, Methodology, Investigation, Formal analysis, Data curation, Conceptualization. **R. Cabrera-Rubio:** Writing – review & editing, Writing – original draft, Methodology, Investigation, Funding acquisition, Formal analysis, Data curation. **F. López-Picón:** Methodology, Investigation, Funding acquisition, Formal analysis, Data curation. **S. Helin:** Methodology, Investigation, Formal analysis, Data curation. **A. Gasparyan:** Methodology, Investigation, Formal analysis, Data curation. **R. Aarnio:** Writing – review & editing, Methodology, Investigation, Formal analysis, Data curation. **J. Rajander:** Methodology, Investigation, Formal analysis, Data curation. **M.C. Collado:** Writing – review & editing, Visualization, Validation, Supervision, Resources, Project administration, Methodology, Funding acquisition, Formal analysis, Data curation, Conceptualization. **Manzanares Jorge:** Writing – review & editing, Visualization, Validation, Supervision, Resources, Project administration, Funding acquisition, Formal analysis, Data curation, Conceptualization.

Declaration of Competing Interest

The authors declare that they have no known competing financial interests or personal relationships that could have appeared to influence the work reported in this paper.

Acknowledgements

This work was supported by grants funded by the Ministry of Health and the National Institute of Health Carlos III (ISCIII) to J. Manzanares (PI21/00488 and RD21/0009/0008), by "Instituto de Investigación Sanitaria y Biomédica de Alicante" (ISABIAL) to J.M., by the Spanish Ministry of Science and Innovation (MCIN) to M.C.Collado (MAMI Plus-ref. PID2022–139475OB-I00), by the Generalitat Valenciana (GVA) to R. Cabrera-Rubio (Plan GenT project, CDEIGENT 2020–02), and by the MCIN and the State Research Agency (AEI) to the Institute of Agrochemistry and Food Technology (IATA-CSIC) and the Institute of Neurosciences (IN-UMH/CSIC) as Centers of Excellence Accreditation Severo Ochoa (CEX2021–001189-S and CEX2021–001165-S -funded by MCIN/AEI/10.13039/501100011033-, respectively).

Data availability

Data will be made available on request.

References

[1] S. Popova, M.E. Charness, L. Burd, A. Crawford, H.E. Hoyme, R.A.S. Mukherjee, E.P. Riley, E.J. Elliott, Fetal alcohol spectrum disorders, Nat. Rev. Dis. Prim. 9 (1) (2023) 11.
[2] J.C. Okurame, L. Cannon, E. Carter, S. Thomas, E.J. Elliott, L.J. Rice, Fetal alcohol spectrum disorder resources for health professionals: a scoping review protocol, BMJ Open 12 (9) (2022) e065327.
[3] K. Mareckova, R. Marecek, L. Andryskova, M. Brazdil, Y.S. Nikolova, Prenatal exposure to alcohol and its impact on reward processing and substance use in adulthood, Transl. Psychiatry 14 (1) (2024) 220.
[4] K. Hausknecht, Y.L. Shen, R.X. Wang, S. Haj-Dahmane, R.Y. Shen, Prenatal ethanol exposure persistently alters endocannabinoid signaling and endocannabinoid-mediated excitatory synaptic plasticity in ventral tegmental area dopamine neurons, J. Neurosci. 37 (24) (2017) 5798–5808.
[5] M.C. Fabio, S.M. March, J.C. Molina, M.E. Nizhnikov, N.E. Spear, R.M. Pautassi, Prenatal ethanol exposure increases ethanol intake and reduces c-Fos expression in infralimbic cortex of adolescent rats, Pharm. Biochem Behav. 103 (4) (2013) 842–852.
[6] L.C. Ornelas, E.W. Fish, J.C. Dooley, M. Carroll, S.E. Parnell, J. Besheer, The impact of prenatal alcohol, synthetic cannabinoid and co-exposure on behavioral adaptations in adolescent offspring and alcohol self-administration in adulthood, Neurotoxicol Teratol. 102 (2024) 107341.
[7] X. Zeng, Y. Cai, M. Wu, H. Chen, M. Sun, H. Yang, An overview of current advances in perinatal alcohol exposure and pathogenesis of fetal alcohol spectrum disorders, J. Neurodev. Disord. 16 (1) (2024) 20.
[8] J.R. Wozniak, E.P. Riley, M.E. Charness, Clinical presentation, diagnosis, and management of fetal alcohol spectrum disorder, Lancet Neurol. 18 (8) (2019) 760–770.
[9] N.J. Murawski, E.M. Moore, J.D. Thomas, E.P. Riley, Advances in diagnosis and treatment of fetal alcohol spectrum disorders: from animal models to human studies, Alcohol Res 37 (1) (2015) 97–108.
[10] B.S. Basavarajappa, Fetal alcohol spectrum disorder: potential role of endocannabinoids signaling, Brain Sci. 5 (4) (2015) 456–493.
[11] B.L. Hungund, Drinking during pregnancy: potential role of endocannabinoid signaling in fetal alcohol effects, World J. Neurol. 7 (1) (2017) 1–5.
[12] A. Viudez-Martinez, M.S. Garcia-Gutierrez, J. Medrano-Relinque, C.M. Navarron, F. Navarrete, J. Manzanares, Cannabidiol does not display drug abuse potential in mice behavior, Acta Pharm. Sin. 40 (3) (2019) 358–364.
[13] C. Ibeas Bih, T. Chen, A.V. Nunn, M. Bazelot, M. Dallas, B.J. Whalley, Molecular targets of cannabidiol in neurological disorders, Neurotherapeutics 12 (4) (2015) 699–730.
[14] N. Martinez Naya, J. Kelly, G. Corna, M. Golino, A. Abbate, S. Toldo, Molecular and cellular mechanisms of action of cannabidiol, Molecules 28 (16) (2023).
[15] M.S. Garcia-Gutierrez, F. Navarrete, A. Gasparyan, A. Austrich-Olivares, F. Sala, J. Manzanares, Cannabidiol: a potential new alternative for the treatment of anxiety, depression, and psychotic disorders, Biomolecules 10 (11) (2020).
[16] K. Han, J.Y. Wang, P.Y. Wang, Y.C. Peng, Therapeutic potential of cannabidiol (CBD) in anxiety disorders: a systematic review and meta-analysis, Psychiatry Res 339 (2024) 116049.
[17] Y. Miao, F. Zhao, W. Guan, A novel insight into the antidepressant effect of cannabidiol: possible involvement of the 5-HT1A, CB1, GPR55, and PPARgamma receptors, Int J. Neuropsychopharmacol. 28 (2) (2025).
[18] M.S. Garcia-Gutierrez, D. Navarro, A. Austrich-Olivares, J. Manzanares, Unveiling behavioral and molecular neuroadaptations related to the antidepressant action of cannabidiol in the unpredictable chronic mild stress model, Front Pharm. 14 (2023) 1171646.
[19] S.M. Tambe, S. Mali, P.D. Amin, M. Oliveira, Neuroprotective potential of cannabidiol: molecular mechanisms and clinical implications, J. Integr. Med 21 (3) (2023) 236–244.
[20] M.M. Aychman, D.L. Goldman, J.S. Kaplan, Cannabidiol's neuroprotective properties and potential treatment of traumatic brain injuries, Front Neurol. 14 (2023) 1087011.
[21] F. Navarrete, M.S. Garcia-Gutierrez, A. Gasparyan, A. Austrich-Olivares, J. Manzanares, Role of cannabidiol in the therapeutic intervention for substance use disorders, Front Pharm. 12 (2021) 626010.
[22] V. Paulus, J. Billieux, A. Benyamina, L. Karila, Cannabidiol in the context of substance use disorder treatment: a systematic review, Addict. Behav. 132 (2022) 107360.

[23] A. Viudez-Martinez, M.S. Garcia-Gutierrez, C.M. Navarron, M.I. Morales-Calero, F. Navarrete, A.I. Torres-Suarez, J. Manzanares, Cannabidiol reduces ethanol consumption, motivation and relapse in mice, Addict. Biol. 23 (1) (2018) 154–164.
[24] A. Viudez-Martinez, M.S. Garcia-Gutierrez, A.I. Fraguas-Sanchez, A.I. Torres-Suarez, J. Manzanares, Effects of cannabidiol plus naltrexone on motivation and ethanol consumption, Br. J. Pharm. 175 (16) (2018) 3369–3378.
[25] P. Maccioni, J. Bratzu, M.A.M. Carai, G. Colombo, G.L. Gessa, Reducing effect of cannabidiol on alcohol self-administration in sardinian alcohol-preferring rats, Cannabis Cannabinoid Res 7 (2) (2022) 161–169.
[26] S. Dirik, M.R. Doyle, C.P. Wood, P. Campo, A.R. Martinez, M. Fannon, M. G. Balaguer, S. Seely, B.A. Montoya, G.M.R. Cook, G.M. Palermo, J. Lin, M.D. Sist, P.K. Naghshineh, Z. Lan, S. Rahman, R. Suhandynata, P. Schweitzer, M. Kallupi, G. de Guglielmo, Cannabidiol mitigates alcohol dependence and withdrawal with neuroprotective effects in the basolateral amygdala and striatum, Neuropsychopharmacology (2025).
[27] A. Gasparyan, D. Navarro, F. Navarrete, A. Austrich-Olivares, E.R. Scoma, V. D. Hambardikar, G.B. Acosta, M.E. Solesio, J. Manzanares, Cannabidiol repairs behavioral and brain disturbances in a model of fetal alcohol spectrum disorder, Pharm. Res 188 (2023) 106655.
[28] A. Garcia-Baos, X. Puig-Reyne, O. Garcia-Algar, O. Valverde, Cannabidiol attenuates cognitive deficits and neuroinflammation induced by early alcohol exposure in a mice model, Biomed. Pharm. 141 (2021) 111813.
[29] J.F. Cryan, K.J. O'Riordan, C.S.M. Cowan, K.V. Sandhu, T.F.S. Bastiaanssen, M. Boehme, M.G. Codagnone, S. Cussotto, C. Fulling, A.V. Golubeva, K. E. Guzzetta, M. Jaggar, C.M. Long-Smith, J.M. Lyte, J.A. Martin, A. Molinero-Perez, G. Moloney, E. Morelli, E. Morillas, R. O'Connor, J.S. Cruz-Pereira, V. L. Peterson, K. Rea, N.L. Ritz, E. Sherwin, S. Spichak, E.M. Teichman, M. van de Wouw, A.P. Ventura-Silva, S.E. Wallace-Fitzsimons, N. Hyland, G. Clarke, T. G. Dinan, The Microbiota-Gut-Brain Axis, Physiol. Rev. 99 (4) (2019) 1877–2013.
[30] E. Schneider, K.J. O'Riordan, G. Clarke, J.F. Cryan, Feeding gut microbes to nourish the brain: unravelling the diet-microbiota-gut-brain axis, Nat. Metab. 6 (8) (2024) 1454–1478.
[31] K. Socala, U. Doboszewska, A. Szopa, A. Serefko, M. Wlodarczyk, A. Zielinska, E. Poleszak, J. Fichna, P. Wlaz, The role of microbiota-gut-brain axis in neuropsychiatric and neurological disorders, Pharm. Res 172 (2021) 105840.
[32] Q. Wang, Q. Yang, X. Liu, The microbiota-gut-brain axis and neurodevelopmental disorders, Protein Cell 14 (10) (2023) 762–775.
[33] A. Parlesak, C. Schafer, T. Schutz, J.C. Bode, C. Bode, Increased intestinal permeability to macromolecules and endotoxemia in patients with chronic alcohol abuse in different stages of alcohol-induced liver disease, J. Hepatol. 32 (5) (2000) 742–747.
[34] S. Leclercq, S. Matamoros, P.D. Cani, A.M. Neyrinck, F. Jamar, P. Starkel, K. Windey, V. Tremaroli, F. Backhed, K. Verbeke, P. de Timary, N.M. Delzenne, Intestinal permeability, gut-bacterial dysbiosis, and behavioral markers of alcohol-dependence severity, Proc. Natl. Acad. Sci. USA 111 (42) (2014) E4485–E4493.
[35] X. Pan, A. Guo, K. Guan, C. Chen, S. Xu, Y. Tang, X. Li, Z. Huang, Lactobacillus rhamnosus GG attenuates depression-like behaviour and cognitive deficits in chronic ethanol exposure mice by down-regulating systemic inflammatory factors, Addict. Biol. 29 (11) (2024) e13445.
[36] H. Wei, C. Yu, C. Zhang, Y. Ren, L. Guo, T. Wang, F. Chen, Y. Li, X. Zhang, H. Wang, J. Liu, Butyrate ameliorates chronic alcoholic central nervous damage by suppressing microglia-mediated neuroinflammation and modulating the microbiome-gut-brain axis, Biomed. Pharm. 160 (2023) 114308.
[37] T.S. Bodnar, G. Ainsworth-Cruickshank, V. Billy, L. Wegener Parfrey, J. Weinberg, C. Raineki, Alcohol consumption during pregnancy differentially affects the fecal microbiota of dams and offspring, Sci. Rep. 14 (1) (2024) 16121.
[38] Y. Wang, T. Xie, Y. Wu, Y. Liu, Z. Zou, J. Bai, Impacts of maternal diet and alcohol consumption during pregnancy on maternal and infant gut microbiota, Biomolecules 11 (3) (2021).
[39] T.S. Bodnar, C. Lee, A. Wong, I. Rubin, L. Wegener Parfrey, J. Weinberg, Evidence for long-lasting alterations in the fecal microbiota following prenatal alcohol exposure, Alcohol Clin. Exp. Res 46 (4) (2022) 542–555.
[40] E. Org, M. Mehrabian, B.W. Parks, P. Shipkova, X. Liu, T.A. Drake, A.J. Lusis, Sex differences and hormonal effects on gut microbiota composition in mice, Gut Microbes 7 (4) (2016) 313–322.
[41] J.G. Markle, D.N. Frank, S. Mortin-Toth, C.E. Robertson, L.M. Feazel, U. Rolle-Kampczyk, M. von Bergen, K.D. McCoy, A.J. Macpherson, J.S. Danska, Sex differences in the gut microbiome drive hormone-dependent regulation of autoimmunity, Science 339 (6123) (2013) 1084–1088.
[42] N. Percie du Sert, V. Hurst, A. Ahluwalia, S. Alam, M.T. Avey, M. Baker, W. J. Browne, A. Clark, I.C. Cuthill, U. Dirnagl, M. Emerson, P. Garner, S.T. Holgate, D.W. Howells, N.A. Karp, S.E. Lazic, K. Lidster, C.J. MacCallum, M. Macleod, E. J. Pearl, O.H. Petersen, F. Rawle, P. Reynolds, K. Rooney, E.S. Sena, S. D. Silberberg, T. Steckler, H. Wurbel, The ARRIVE guidelines 2.0: Updated guidelines for reporting animal research, Br. J. Pharm. 177 (16) (2020) 3617–3624.
[43] N.B. Nabulsi, J. Mercier, D. Holden, S. Carre, S. Najafzadeh, M.C. Vandergeten, S. F. Lin, A. Deo, N. Price, M. Wood, T. Lara-Jaime, F. Montel, M. Laruelle, R. E. Carson, J. Hannestad, Y. Huang, Synthesis and Preclinical Evaluation of 11C-UCB-J as a PET Tracer for Imaging the Synaptic Vesicle Glycoprotein 2A in the Brain, J. Nucl. Med 57 (5) (2016) 777–784.
[44] K. Varnas, V. Stepanov, C. Halldin, Autoradiographic mapping of synaptic vesicle glycoprotein 2A in non-human primate and human brain, Synapse 74 (10) (2020) e22157.
[45] L. Farde, H. Hall, E. Ehrin, G. Sedvall, Quantitative analysis of D2 dopamine receptor binding in the living human brain by PET, Science 231 (4735) (1986) 258–261.
[46] Paxinos G., Franklin K.B.J. The mouse brain in stereotaxic coordinates. Amsterdam; Boston: Elsevier Academic Press; 2004.
[47] M. Palkovits, Punch sampling biopsy technique, Methods Enzym. 103 (1983) 368–376.
[48] K.J. Livak, T.D. Schmittgen, Analysis of relative gene expression data using real-time quantitative PCR and the 2(-Delta Delta C(T)) Method, Methods 25 (4) (2001) 402–408.
[49] S. Chen, Y. Zhou, Y. Chen, J. Gu, fastp: an ultra-fast all-in-one FASTQ preprocessor, Bioinformatics 34 (17) (2018) i884–i890.
[50] E. Aronesty, Comparison of Sequencing Utility Programs, Open Bioinforma. J. 7 (2013) 1–8.
[51] R.C. Edgar, Search and clustering orders of magnitude faster than BLAST, Bioinformatics 26 (19) (2010) 2460–2461.
[52] R. Schmieder, R. Edwards, Fast identification and removal of sequence contamination from genomic and metagenomic datasets, PLoS One 6 (3) (2011) e17288.
[53] R.C. Edgar, UNOISE2: improved error-correction for Illumina 16S and ITS amplicon sequencing, bioRxiv (2016).
[54] J.G. Caporaso, J. Kuczynski, J. Stombaugh, K. Bittinger, F.D. Bushman, E. K. Costello, N. Fierer, A.G. Pena, J.K. Goodrich, J.I. Gordon, G.A. Huttley, S. T. Kelley, D. Knights, J.E. Koenig, R.E. Ley, C.A. Lozupone, D. McDonald, B. D. Muegge, M. Pirrung, J. Reeder, J.R. Sevinsky, P.J. Turnbaugh, W.A. Walters, J. Widmann, T. Yatsunenko, J. Zaneveld, R. Knight, QIIME allows analysis of high-throughput community sequencing data, Nat. Methods 7 (5) (2010) 335–336.
[55] N.A. Bokulich, B.D. Kaehler, J.R. Rideout, M. Dillon, E. Bolyen, R. Knight, G. A. Huttley, J. Gregory Caporaso, Optimizing taxonomic classification of marker-gene amplicon sequences with QIIME 2's q2-feature-classifier plugin, Microbiome 6 (1) (2018) 90.
[56] J.R. Cole, Q. Wang, J.A. Fish, B. Chai, D.M. McGarrell, Y. Sun, C.T. Brown, A. Porras-Alfaro, C.R. Kuske, J.M. Tiedje, Ribosomal Database Project: data and tools for high throughput rRNA analysis, Nucleic Acids Res 42 (Database) (2014) D633–D642.
[57] K. Katoh, D.M. Standley, MAFFT multiple sequence alignment software version 7: improvements in performance and usability, Mol. Biol. Evol. 30 (4) (2013) 772–780.
[58] M.N. Price, P.S. Dehal, A.P. Arkin, FastTree 2–approximately maximum-likelihood trees for large alignments, PLoS One 5 (3) (2010) e9490.
[59] F. Navarrete, G. Rubio, J. Manzanares, Effects of naltrexone plus topiramate on ethanol self-administration and tyrosine hydroxylase gene expression changes, Addict. Biol. 19 (5) (2014) 862–873.
[60] M.S. Garcia-Gutierrez, F. Navarrete, A. Aracil, A. Bartoll, I. Martinez-Gras, J. L. Lanciego, G. Rubio, J. Manzanares, Increased vulnerability to ethanol consumption in adolescent maternal separated mice, Addict. Biol. 21 (4) (2016) 847–858.
[61] A. Orru, D. Fujani, C. Cassina, M. Conti, A. Di Clemente, L. Cervo, Operant, oral alcoholic beer self-administration by C57BL/6J mice: effect of BHF177, a positive allosteric modulator of GABA(B) receptors, Psychopharmacol. (Berl.) 222 (4) (2012) 685–700.
[62] C. Cohen, O. Curet, G. Perrault, D.J. Sanger, Reduction of oral ethanol self-administration in rats by monoamine oxidase inhibitors, Pharm. Biochem Behav. 64 (3) (1999) 535–539.
[63] L.D. Middaugh, B.M. Kelley, Operant ethanol reward in C57BL/6 mice: influence of gender and procedural variables, Alcohol 17 (3) (1999) 185–194.
[64] K.A. Grant, H.H. Samson, The induction of oral ethanol self-administration by contingent ethanol delivery, Drug Alcohol Depend. 16 (4) (1986) 361–368.
[65] P.J. McMurdie, S. Holmes, phyloseq: an R package for reproducible interactive analysis and graphics of microbiome census data, PLoS One 8 (4) (2013) e61217.
[66] Oksanen J., Simpson G., Blanchet F., Kindt R., Legendre P., Minchin P., O'Hara R., Solymos P., Stevens M., Szoecs E., Wagner H., Barbour M., Bedward M., Bolker B., Borcard D., Borman T., Carvalho G., Chirico M., De Caceres M., Durand S., Evangelista H., FitzJohn R., Friendly M., Furneaux B., Hannigan G., Hill M., Lahti L., McGlinn D., Ouellette M., Ribeiro Cunha E., Smith T., Stier A., Ter Braak C., Weedon J vegan: Community Ecology Package. 2013. R package version 2.7-0 hgcvv, https://vegandevs.github.io/vegan/. vegan: Community Ecology Package. R package version 2.7-0. Available from: https://github.com/vegandevs/vegan, https://vegandevs.github.io/vegan/.
[67] H. Zou, T. Hastie, Regularization and Variable Selection Via the Elastic Net, J. R. Stat. Soc. Ser. B Stat. Methodol. 67 (2) (2025) 301–320.
[68] J. Rivera-Pinto, J.J. Egozcue, V. Pawlowsky-Glahn, R. Paredes, M. Noguera-Julian, M.L. Calle, Balances: a New Perspective for Microbiome Analysis, mSystems 3 (4) (2018).
[69] K. Inomata, F. Nasu, H. Tanaka, Decreased density of synaptic formation in the frontal cortex of neonatal rats exposed to ethanol in utero, Int J. Dev. Neurosci. 5 (5-6) (1987) 455–460.
[70] J.H. Sliwowska, J.M. Barker, C.K. Barha, N. Lan, J. Weinberg, L.A. Galea, Stress-induced suppression of hippocampal neurogenesis in adult male rats is altered by prenatal ethanol exposure, Stress 13 (4) (2010) 301–313.
[71] K.A. Uban, J.H. Sliwowska, S. Lieblich, L.A. Ellis, W.K. Yu, J. Weinberg, L. A. Galea, Prenatal alcohol exposure reduces the proportion of newly produced neurons and glia in the dentate gyrus of the hippocampus in female rats, Horm. Behav. 58 (5) (2010) 835–843.

[72] L. An, T. Zhang, Spatial cognition and sexually dimorphic synaptic plasticity balance impairment in rats with chronic prenatal ethanol exposure, Behav. Brain Res 256 (2013) 564–574.
[73] H.M. Sickmann, A.R. Patten, K. Morch, S. Sawchuk, C. Zhang, R. Parton, L. Szlavik, B.R. Christie, Prenatal ethanol exposure has sex-specific effects on hippocampal long-term potentiation, Hippocampus 24 (1) (2014) 54–64.
[74] A.K. Titterness, B.R. Christie, Prenatal ethanol exposure enhances NMDAR-dependent long-term potentiation in the adolescent female dentate gyrus, Hippocampus 22 (1) (2012) 69–81.
[75] Y. Cai, J.C. Wu, Y. Huang, X.F. Yu, F.H. Liu, Z.W. Chen, D.P. Gao, Impaired cognitive function and altered dendritic morphology of hippocampal neurons in a mouse model of fetal alcohol spectrum disorder, Behav. Brain Res 490 (2025) 115633.
[76] M.C. Fabio, L.M. Vivas, R.M. Pautassi, Prenatal ethanol exposure alters ethanol-induced Fos immunoreactivity and dopaminergic activity in the mesocorticolimbic pathway of the adolescent brain, Neuroscience 301 (2015) 221–234.
[77] S. Randall, J.H. Hannigan, In utero alcohol and postnatal methylphenidate: locomotion and dopamine receptors, Neurotoxicol Teratol. 21 (5) (1999) 587–593.
[78] S. Bariselli, Y. Mateo, N. Reuveni, D.M. Lovinger, Gestational ethanol exposure impairs motor skills in female mice through dysregulated striatal dopamine and acetylcholine function, Neuropsychopharmacology 48 (12) (2023) 1808–1820.
[79] E.A. Bartlett, F. Zanderigo, D. Shieh, J. Miller, P. Hurley, H. Rubin-Falcone, M. A. Oquendo, M.E. Sublette, R.T. Ogden, J.J. Mann, Serotonin transporter binding in major depressive disorder: impact of serotonin system anatomy, Mol. Psychiatry 27 (8) (2022) 3417–3424.
[80] J.A. Morgan, G. Singhal, F. Corrigan, E.J. Jaehne, M.C. Jawahar, J. Breen, S. Pederson, B.T. Baune, Ceasing exercise induces depression-like, anxiety-like, and impaired cognitive-like behaviours and altered hippocampal gene expression, Brain Res Bull. 148 (2019) 118–130.
[81] A. Gasparyan, F. Navarrete, J. Manzanares, Cannabidiol and Sertraline Regulate Behavioral and Brain Gene Expression Alterations in an Animal Model of PTSD, Front Pharm. 12 (2021) 694510.
[82] M. Willeit, H.H. Sitte, N. Thierry, K. Michalek, N. Praschak-Rieder, P. Zill, D. Winkler, W. Brannath, M.B. Fischer, B. Bondy, S. Kasper, E.A. Singer, Enhanced serotonin transporter function during depression in seasonal affective disorder, Neuropsychopharmacology 33 (7) (2008) 1503–1513.
[83] H.M. Hwang, Y.I. Kawasawa, A. Basha, S. Mohammad, M. Ito, K. Hashimoto-Torii, Fatty acid metabolism changes in association with neurobehavioral deficits in animal models of fetal alcohol spectrum disorders, Commun. Biol. 6 (1) (2023) 736.
[84] D. Upreti, S.K. Rouzer, A. Bowring, E. Labbe, R. Kumar, R.C. Miranda, A. H. Mahnke, Microbiota and nutrition as risk and resiliency factors following prenatal alcohol exposure, Front Neurosci. 17 (2023) 1182635.
[85] R.H. McMahan, H.J. Hulsebus, K.M. Najarro, L.E. Giesy, D.N. Frank, E.J. Kovacs, Changes in gut microbiome correlate with intestinal barrier dysfunction and inflammation following a 3-day ethanol exposure in aged mice, Alcohol 107 (2023) 136–143.
[86] B.J. Parker, P.A. Wearsch, A.C.M. Veloo, A. Rodriguez-Palacios, The Genus Alistipes: Gut Bacteria With Emerging Implications to Inflammation, Cancer, and Mental Health, Front Immunol. 11 (2020) 906.
[87] M.S. Virdee, N. Saini, C.D. Kay, A.P. Neilson, S.T.C. Kwan, K.K. Helfrich, S. M. Mooney, S.M. Smith, An enriched biosignature of gut microbiota-dependent metabolites characterizes maternal plasma in a mouse model of fetal alcohol spectrum disorder, Sci. Rep. 11 (1) (2021) 248.
[88] J.F. Cryan, T.G. Dinan, Mind-altering microorganisms: the impact of the gut microbiota on brain and behaviour, Nat. Rev. Neurosci. 13 (10) (2012) 701–712.
[89] A. Everard, C. Belzer, L. Geurts, J.P. Ouwerkerk, C. Druart, L.B. Bindels, Y. Guiot, M. Derrien, G.G. Muccioli, N.M. Delzenne, W.M. de Vos, P.D. Cani, Cross-talk between Akkermansia muciniphila and intestinal epithelium controls diet-induced obesity, Proc. Natl. Acad. Sci. USA 110 (22) (2013) 9066–9071.
[90] C. Silvestri, E. Pagano, S. Lacroix, T. Venneri, C. Cristiano, A. Calignano, O. A. Parisi, A.A. Izzo, V. Di Marzo, F. Borrelli, Fish Oil, Cannabidiol and the Gut Microbiota: An Investigation in a Murine Model of Colitis, Front Pharm. 11 (2020) 585096.
[91] Z.Z. Al-Ghezi, P.B. Busbee, H. Alghetaa, P.S. Nagarkatti, M. Nagarkatti, Combination of cannabinoids, delta-9-tetrahydrocannabinol (THC) and cannabidiol (CBD), mitigates experimental autoimmune encephalomyelitis (EAE) by altering the gut microbiome, Brain Behav. Immun. 82 (2019) 25–35.
[92] X. Wang, L. Li, C. Bian, M. Bai, H. Yu, H. Gao, J. Zhao, C. Zhang, R. Zhao, Alterations and correlations of gut microbiota, fecal, and serum metabolome characteristics in a rat model of alcohol use disorder, Front Microbiol 13 (2022) 1068825.
[93] K. Amir Hamzah, L.M. Toms, N. Kucharski, J. Orr, N.P. Turner, P. Hobson, D. S. Nichols, L.J. Ney, Sex-dimorphism in human serum endocannabinoid and n-acyl ethanolamine concentrations across the lifespan, Sci. Rep. 13 (1) (2023) 23059.
[94] L. Wilmes, V. Caputi, T.F.S. Bastiaanssen, J.M. Collins, F. Crispie, P.D. Cotter, T. G. Dinan, J.F. Cryan, G. Clarke, S.M. O'Mahony, Sex specific gut-microbiota signatures of resilient and comorbid gut-brain phenotypes induced by early life stress, Neurobiol. Stress 33 (2024) 100686.
[95] G. Chevalier, E. Siopi, L. Guenin-Mace, M. Pascal, T. Laval, A. Rifflet, I.G. Boneca, C. Demangel, B. Colsch, A. Pruvost, E. Chu-Van, A. Messager, F. Leulier, G. Lepousez, G. Eberl, P.M. Lledo, Effect of gut microbiota on depressive-like behaviors in mice is mediated by the endocannabinoid system, Nat. Commun. 11 (1) (2020) 6363.
[96] M.E. Nizhnikov, J.C. Molina, E.I. Varlinskaya, N.E. Spear, Prenatal ethanol exposure increases ethanol reinforcement in neonatal rats, Alcohol Clin. Exp. Res 30 (1) (2006) 34–45.
[97] R.M. Pautassi, M.E. Nizhnikov, N.E. Spear, J.C. Molina, Prenatal ethanol exposure leads to greater ethanol-induced appetitive reinforcement, Alcohol 46 (6) (2012) 585–593.
[98] M.C. Fabio, A.F. Macchione, M.E. Nizhnikov, R.M. Pautassi, Prenatal ethanol increases ethanol intake throughout adolescence, alters ethanol-mediated aversive learning, and affects mu but not delta or kappa opioid receptor mRNA expression, Eur. J. Neurosci. 41 (12) (2015) 1569–1579.
[99] E. Barbier, H. Houchi, V. Warnault, O. Pierrefiche, M. Daoust, M. Naassila, Effects of prenatal and postnatal maternal ethanol on offspring response to alcohol and psychostimulants in long evans rats, Neuroscience 161 (2) (2009) 427–440.
[100] O.V. Torres, E.M. Walker, B.S. Beas, L.E. O'Dell, Female rats display enhanced rewarding effects of ethanol that are hormone dependent, Alcohol Clin. Exp. Res 38 (1) (2014) 108–115.
[101] G. Koren, R. Cohen, O. Sachs, Use of cannabis in fetal alcohol spectrum disorder, Cannabis Cannabinoid Res 6 (1) (2021) 74–76.